Table 2. Association between the *COQ2* V393A Variant and Sporadic Multiple-System Atrophy in the Japanese Series.*

V343A Variant†‡	Patients with Multiple-System Atrophy						Patients with Other Neurologic Diseases		
	Patients (N=363)	Tier 1 Controls (N=520)	Comparison with Tier 1		Tier 2 Controls (N=2383)	Comparison with Tier 2	Alzheimer's Disease (N=2728)	Parkinson's Disease (N=659)	ALS (N=634)
			odds ratio (95% CI)	*P value*		*odds ratio (95% CI)*	*P value*			
Allele frequency — no./total no. (%)	35/726 (4.8)	17/1040 (1.6)	3.05 (1.65–5.85)	1.5×10^{-4}	106/4766 (2.2)	2.23 (1.46–3.32)	6.0×10^{-5}	109/5456 (2.0)	33/1318 (2.5)	31/1268 (2.4)
Heterozygous — no.	31	17			106			105	33	31
Homozygous — no.	2	0			0			2	0	0

* Odds ratios and P values are for the comparisons between patients with multiple-system atrophy and each of the two groups of controls (tier 1 and tier 2). ALS denotes amyotrophic lateral sclerosis, and CI confidence interval.

† In the combined series of Japanese, European, and North American participants, functionally deleterious variants P99H, S107T, R119H, I147T, P157S, S163F, T317A, S347C, and R387Q (as determined on yeast complementation assay) were found in 8 of 1516 alleles (0.53%) in patients with multiple-system atrophy, as compared with 1 of 2258 alleles (0.05%) in controls (odds ratio, 11.97; 95% CI, 1.60 to 531.5; P=0.004).

of genomic DNA from the parents were unavailable. We found that 29 patients with multiple-system atrophy and 17 controls were heterozygous for the V393A variant. In addition, we detected four novel heterozygous variants: two in patients with multiple-system atrophy (P157S [c.469C→T] and S163F [c.488C→T] and two in controls (P72L [c.215C→T] and N386H ([c.1156A→C]).

Of the *COQ2* variants, the V393A variant is relatively common in the Japanese population. As shown in Table 2, we found that the V393A allele occurred in 35 of 726 alleles (4.8%) from Japanese patients with multiple-system atrophy and in 17 of 1040 alleles (1.6%) from Japanese controls (odds ratio for patients with multiple-system atrophy, 3.05; 95% confidence interval [CI], 1.65 to 5.85; $P=1.5\times10^{-4}$). Genotyping in the second series of 2383 Japanese controls showed that the V393A variant had an allele frequency of 2.2% (106 of 4766 alleles; odds ratio, 2.23; 95% CI, 1.46 to 3.32; $P=6.0\times10^{-5}$). Genotyping Japanese persons with other neurodegenerative diseases revealed that the V393A allele frequencies were 2.0% (109 of 5456 alleles) among patients with Alzheimer's disease, 2.5% (33 of 1318 alleles) among those with Parkinson's disease, and 2.4% (31 of 1268 alleles) among those with ALS. These allele frequencies did not differ significantly from those in the first or second set of controls, confirming the specificity of the V393A variant in patients with multiple-system atrophy. Two patients with Alzheimer's disease who were found to carry homozygous V393A mutations did not show any signs of parkinsonism, cerebellar ataxia, or autonomic dysfunction.

We then performed genotyping in the European and North American series of patients with multiple-system atrophy. In the European series, we found four singleton *COQ2* variants (encoding amino acid substitutions F79L [c.235T→C], S1077T [c.320G→C], T317A [c.949A→G], and S347C [c.1039A→T]) among the patients, whereas none of the controls had any variants in *COQ2*. In the North American series, we found one variant (P99H [c.296C→A]) in a patient with multiple-system atrophy and one variant (R119H [c.356G→A]) in a control (Table 1). At the time of recruitment for the study, the carrier of R119H, who was 60 years old, had no signs of parkinsonism, cerebellar ataxia, or autonomic dysfunction, but this participant was unavailable for follow-up assessment. Intriguingly, the V393A

variant, a relatively common variant in the Japanese population, was not observed in patients with multiple-system atrophy or controls in either the European or the North American series.

FUNCTIONAL ANALYSIS OF MUTANT COQ2

To determine the functional effect of each variant on the mitochondrial aerobic energy production in which coenzyme Q_{10} plays an essential

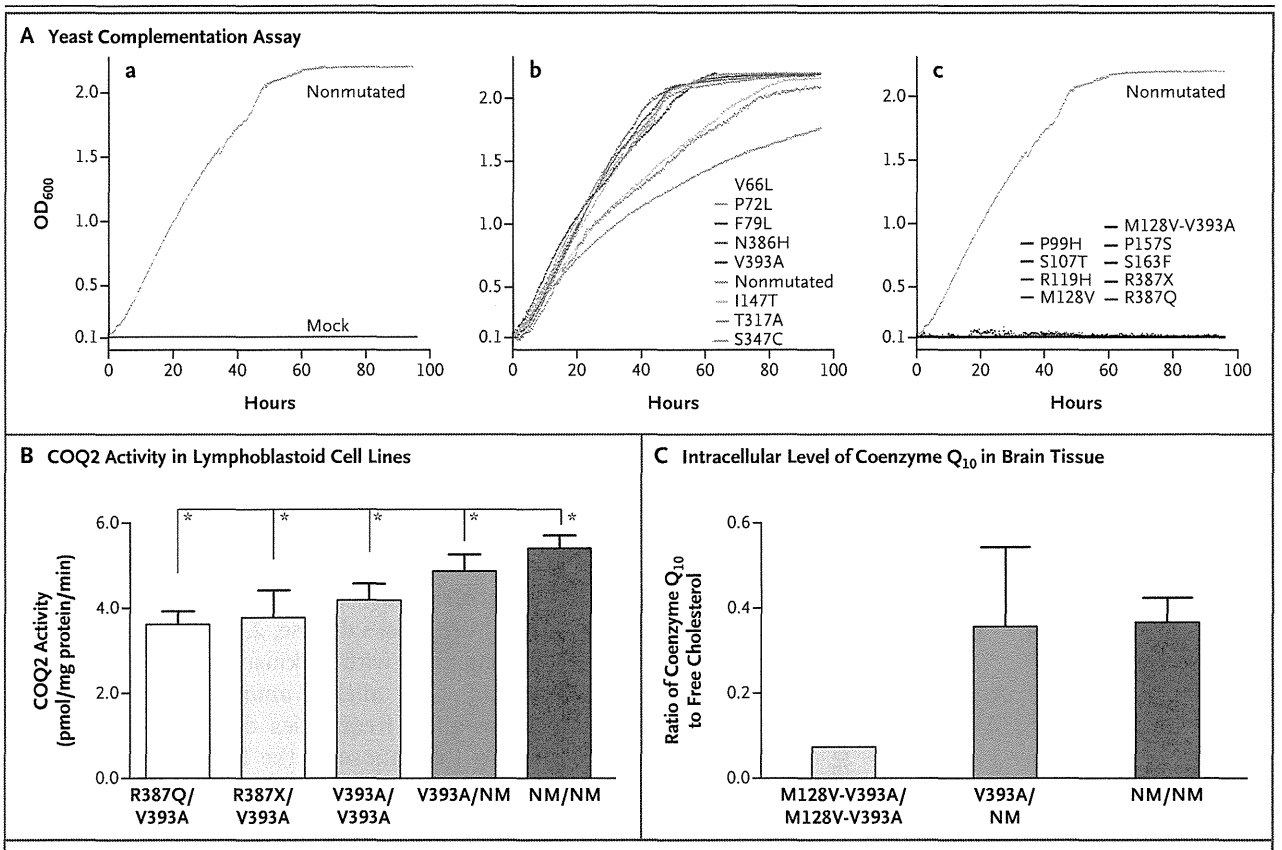

Figure 2. Functional Analysis of *COQ2* Variants.

Panel A shows the results of a yeast complementation assay, including the growth curves of the yeast *coq2*-null mutants transformed with the pAUR123 vector containing the nonmutated (NM) human *COQ2* complementary DNA (cDNA) or mock vector (subpanel a) and those transformed with the AUR123 vector containing different versions of human *COQ2* cDNA (encoding the substitutions V66L, P72L, F79L, N386H, V393A, I147T, T317A, and S347C) (subpanel b). Transformants carrying a *COQ2* allele encoding the I147T, T317A, or S347C substitution show considerably lower growth rates than nonmutated *COQ2*, which still shows a higher growth rate than the *coq2*-null strain (mildly deleterious). Transformants carrying a *COQ2* allele encoding the V66L, P72L, F79L, N386H, or V393A substitution show growth rates similar to that of nonmutated *COQ2*. The *coq2*-null mutants transformed with the pAUR123 vector containing different versions of human *COQ2* cDNA (P99H, S107T, R119H, M128V, M128V-V393A, P157S, S163F, R387X, or R387Q) show severely decreased respiration-dependent growth rates, as does the *coq2*-null strain (severely deleterious) (subpanel c). Each yeast strain was pregrown in yeast extract peptone dextrose (YPD) medium, diluted to an optical density of a sample measured at a wavelength of 600 nm (OD_{600}) of 0.1, and then incubated in yeast extract peptone glycerol (YPG) medium at 23°C with shaking at a rate of 200 rotations per minute for 4 days. OD_{600} was measured every 10 minutes. The experiments were conducted in quadruplicate, and the mean OD_{600} was plotted against the incubation time. Panel B shows COQ2 activity in lymphoblastoid cell lines, as determined by measuring the incorporation of radioactive parahydroxybenzoate (PHB) into decaprenyl-PHB. COQ2 activity was measured in lymphoblastoid cell lines from each patient with multiple-system atrophy carrying *COQ2* variants (encoding R387Q/V393A, R387X/V393A, V393A/V393A, or V393A/NM) and from a control without variants. The mean values from nine independent experiments are shown. T bars indicate standard deviations. Group comparisons were performed with the use of the Kruskal–Wallis test, followed by the Steel test. Asterisks indicate $P<0.05$ for the comparison with a control sample (nonmutated *COQ2* genotype). Panel C shows intracellular levels of coenzyme Q_{10} in frozen cerebellum samples obtained from three patients with multiple-system atrophy (one who was homozygous for M128V-V393A and two who were heterozygous for V393A) and from three controls. Brain-tissue samples weighing approximately 100 mg were homogenized in 10 volumes (volume to weight) of 10 mM TRIS–hydrochloric acid (with a pH of 7.4) containing 0.32 M sucrose, 1 mM ethylenediaminetetraacetic acid (EDTA), and 20% sodium dodecyl sulfate (SDS). Coenzyme Q_{10} was then extracted with hexane and ethanol (in a 5:2 ratio according to volume), and the extract was subjected to high-performance liquid chromatography to measure the level of coenzyme Q_{10}, after adjustment for the free (unesterified) cholesterol level.[21]

role in the electron transfer, we carried out functional complementation analysis by transforming the yeast *coq2*-null strain with nonmutated or mutated human *COQ2* cDNA (Fig. 2A). Transformants of the BY4741 Δ*coq2* yeast strain with the mutated *COQ2*, including transformants separately carrying the P99H, S107T, R119H, M128V, M128V-V393A, P157S, S163F, R387Q, and R387X alleles, showed severely decreased growth rates, similar to those observed in the *coq2*-null strain. In addition, transformants with mutated *COQ2*, including those with the variants encoding the I147T, T317A (c.949A→G), and S347C (c.1039A→T) substitutions, showed substantially lower growth rates than those expressing nonmutated *COQ2*, which had a higher growth rate than the *coq2*-null strain (mildly deleterious). The transformants with mutated *COQ2*, including transformants separately carrying the V66L, P72L, F79L, N386H, and V393A alleles, showed growth rates similar to those of the transformants expressing nonmutated *COQ2*. As described above, the yeast strain with M128V-V393A identified in Family 1 showed a severely decreased growth rate, whereas the strain with V393A had a growth rate similar to that of nonmutated *COQ2*, indicating that of the two variants, M128V primarily contributed to the impairment in COQ2 function.

Focusing on the rare variants that were identified in the case–control series (Table 1), we found that nine variants (P99H, S107T, R119H, I147T, P157S, S163F, T317A, S347C, and R387Q) were mildly or severely deleterious. On combining all three series, eight variants (P99H, S107T, I147T, P157S, S163F, T317A, S347C, and R387Q) were identified in 758 patients with multiple-system atrophy, whereas only one variant (R119H) was found in 1129 controls (odds ratio, 11.97; 95% CI, 1.60 to 531.52; P=0.004) (Table 2 footnote). Yeast complementation analysis showed that the F79L variant, identified in a European patient with multiple-system atrophy, did not impair the growth rate. Lymphoblastoid cell lines from this patient were unavailable for further measurement of the activity of mutant COQ2, thus making it difficult to interpret the pathogenicity of this variant.

COQ2 ACTIVITIES IN LYMPHOBLASTOID CELL LINES

We measured COQ2 activities in lymphoblastoid cell lines from patients carrying *COQ2* mutations, when available. We focused on the V393A variant because it is commonly associated with multiple-system atrophy and showed an apparently normal growth rate in the yeast complementation assay. We determined COQ2 activities in lymphoblastoid cell lines with *COQ2* variants R387Q/V393A, R387X/V393A, V393A/V393A, or V393A/NM and in a control without variants. The COQ2 activities in the lymphoblastoid cell lines (V393A/NM) obtained from patients with multiple-system atrophy were significantly lower than those in the control cell lines. The COQ2 activities in the cell lines from patients with multiple-system atrophy carrying two mutated *COQ2* alleles were further decreased (Fig. 2B).

CORRELATIONS BETWEEN GENOTYPE AND PHENOTYPE

The clinical features of patients with sporadic multiple-system atrophy carrying deleterious *COQ2* variants (as determined on yeast complementation assay and COQ2-activity measurement) and those of noncarriers are summarized in Table S5 in the Supplementary Appendix. The mean age at the onset of multiple-system atrophy among carriers was older than that among noncarriers (P=0.002). Among carriers, 34 had subtype C and 5 had subtype P. Among noncarriers, 468 had subtype C and 209 had subtype P. The subtype was unclassified in 42 noncarriers. The ratio of the number of patients with subtype C to the number with subtype P was significantly higher among carriers of *COQ2* variants than among noncarriers (P=0.02).

INTRACELLULAR COENZYME Q_{10} IN LYMPHOBLASTOID CELL LINES

We measured intracellular coenzyme Q_{10} levels in lymphoblastoid cell lines from patients with multiple-system atrophy and controls. The participants were grouped as follows: 3 patients with multiple-system atrophy carrying two variants (R387Q/V393A, R387X/V393A, and V393A/V393A), 16 patients carrying heterozygous V393A, 133 patients without variants, and 76 controls without *COQ2* variants (Table 3). Intracellular levels of coenzyme Q_{10} in lymphoblastoid cell lines from patients with multiple-system atrophy who carried two variant alleles were substantially lower than levels in cell lines from controls without variants. Intracellular coenzyme Q_{10} levels in patients who were heterozygous for V393A and in those without *COQ2* variants were not significantly lower than levels in controls without *COQ2* variants.

Table 3. **Intracellular Levels of Coenzyme Q_{10} in Lymphoblastoid Cell Lines, According to *COQ2* Variant.***

Variable	Patients with Multiple-System Atrophy					Controls
	R387Q/V393A	R387X/V393A	V393A/V393A	V393A/NM	NM/NM	NM/NM
No. of participants with variant	1	1	1	16	133	76
Ratio of coenzyme Q_{10} to free (unesterified) cholesterol†	2.19	2.58	1.86	3.38±0.53	3.41±0.74	3.48±0.75
Coenzyme Q_{10} level as a percentage of mean value in controls — %‡	62.9	74.1	53.4	97.1	98.0	100.0

* Plus–minus values are means ±SD. NM denotes nonmutated.
† The ratio of coenzyme Q_{10} to free (unesterified) cholesterol reflects the intracellular level of coenzyme Q_{10}. Lower values indicate decreased levels of intracellular coenzyme Q_{10}, presumably reflecting decreased biosynthesis of coenzyme Q_{10}. To calculate the ratio, coenzyme Q_{10} was measured in nanomoles per liter and free cholesterol in micromoles per liter.
‡ Lower values indicate decreased levels of intracellular coenzyme Q_{10}, as compared with the mean value in controls, presumably reflecting decreased biosynthesis of coenzyme Q_{10}.

COENZYME Q_{10} IN BRAIN TISSUE

Only a limited number of brain-tissue samples from patients with multiple-system atrophy carrying *COQ2* variants were available. Nevertheless, we measured coenzyme Q_{10} in frozen brain tissues from three patients with *COQ2* variants (one patient who was homozygous for M128V-V393A and two patients with V393A/NM) and from three controls without *COQ2* variants (Fig. 2C). The levels of coenzyme Q_{10} in patients who were homozygous for M128V-V393A were substantially lower than the levels in controls.

DISCUSSION

We identified homozygous or compound heterozygous *COQ2* mutations in two of the six multiplex families with multiple-system atrophy, a finding that suggests a role of these mutations in the pathogenesis of familial disease. We further found that functionally impaired variants in *COQ2* were associated with an increased risk of sporadic disease. In familial cases of multiple-system atrophy, linkage analysis strongly indicated locus heterogeneity in these families, and the identification of the causal variants in the remaining four families will require analyses such as whole-genome sequencing.

We found that a common variant (V393A) and multiple rare variants in *COQ2* were associated with sporadic multiple-system atrophy. The V393A variant was found exclusively in the Japanese participants, with an allele frequency of 1.6 to 2.2%. The allele frequency of V393A in patients with multiple-system atrophy (4.8%) was significantly higher than that in controls (1.6 to 2.2%) with odds ratios of 2.23 to 3.05. The modest risk of multiple-system atrophy that was associated with the common variant V393A suggests that V393A is a susceptibility factor rather than a causal factor for this disease. The odds ratio for the presence of deleterious rare variants was 11.97, which is much larger than that for V393A. Nonetheless, we should consider that these heterozygous variants in *COQ2* are not necessarily causal but rather confer a strong susceptibility to sporadic multiple-system atrophy. Members of Family 1 and Family 12 who carried deleterious variants in the heterozygous state did not have clinical signs of multiple-system atrophy.

The ratio of patients with subtype C multiple-system atrophy to those with subtype P was higher among carriers of deleterious *COQ2* variants than among noncarriers, which suggests that the cerebellum is more vulnerable to compromised COQ2 function than other regions of the central nervous system. Of the *COQ2* variants that we detected, the V393A variant was the most prevalent and was exclusively found in Japanese participants. These findings may in part explain the clinical observations that subtype C is more prevalent than subtype P in the Japanese population[9] but not in the European population[11] or the North American population.[12] However, there were only 35 carriers of deleterious *COQ2* variants among 363 patients with multiple-system atrophy in the Japanese case series. In addition, the clinical presentations of the two patients with familial disease who had the highest mutational load were different: subtype P in the patients in Fam-

ily 1 and subtype C in the patients in Family 12. Thus, the genotypes of *COQ2* do not fully explain the clinical phenotypes.

Previous studies have shown evidence of mitochondrial respiratory-chain dysfunction or oxidative injury in patients with multiple-system atrophy.[22-24] The combination of oxidative stress and overexpression of oligodendroglial α-synuclein has been reported to replicate the characteristics of this disease.[25-28] Our findings suggest that impaired COQ2 activity, which would be predicted to impair the mitochondrial respiratory chain and increase vulnerability to oxidative stress, causes susceptibility to multiple-system atrophy. A primary deficiency of coenzyme Q_{10} that is caused by *COQ2* mutations has been described as an infantile-onset multisystem disorder and a nephropathy in several families.[29,30] The clinical presentation of these affected family members, however, differed markedly from the presentations of patients with multiple-system atrophy, perhaps because the decrease in COQ2 activity associated with the mutations in patients with multiple-system atrophy appears to be milder than that observed in patients with a primary deficiency of coenzyme Q_{10}.

Previous approaches to identifying susceptibility genes have used genomewide association studies or candidate-gene approaches.[31-33] Our identification of rare *COQ2* variants was accomplished by starting with multiplex families and then extending the analysis to patients with sporadic multiple-system atrophy, reflecting an alternative approach to the elucidation of genetic variants with strong effect sizes in an apparently nongenetic disorder.[34]

From the therapeutic viewpoint, oral supplementation with coenzyme Q_{10} may be helpful in treating multiple-system atrophy, particularly for patients with susceptibility-conferring *COQ2* variants. The safety and side-effect profile of high-dose supplementation with coenzyme Q_{10} have been well established.[35,36]

ADDENDUM

Human *COQ2* contains four ATG codons in exon 1. Among the four potential translation initiation codons in exon 1, the protein isoform starting at the fourth ATG codon has been adopted as the canonical sequence of the COQ2 protein in the UniProt database (Q96H96, http://www.uniprot.org/uniprot/Q96H96). In this study, we focused entirely on *COQ2* variants after the fourth ATG codon.

Supported in part by grants from the Japan Society for the Promotion of Science (KAKENHI) (22129001 and 22129002, to Dr. Tsuji); the Ministry of Health, Labor, and Welfare of Japan (H23-Jitsuyoka [Nanbyo]-Ippan-004, to Dr. Tsuji); the Japanese Ministry of Education, Culture, Sports, Science, and Technology; the French Agency for Research (ANR-09-MNPS-032-01/R09148DS, to Drs. Dürr and Brice); Programme Hospitalier de Recherche Clinique (AOM03059/R05129DD, to Drs. Dürr and Brice); Deutsche Forschungsgemeinschaft (Wu 184-6, to Dr. Wüllner); and Deutsche Parkinson Vereinigung (to Dr. Wüllner).

Disclosure forms provided by the authors are available with the full text of this article at NEJM.org.

We thank the staff members of the Radioisotope Center at the University of Tokyo; Keiko Hirayama, Zhenghong Wu, and Mio Takeyama for their support in laboratory experiments; Dr. Kazuyuki Tao, Shinya Uchino, and Manabu Seki for their technical help; Dr. Cecilia Marelli for her clinical input; Drs. Yoshinori Kajimoto and Kokoro Ozaki for providing DNA samples and clinical information; and the DNA and Cell Bank of Centre de Recherche de l'Institut du Cerveau et de la Moelle Épinière (CRICM) in Paris for technical assistance.

APPENDIX

The members of the Multiple System Atrophy Research Collaboration are as follows: Jun Mitsui, M.D., Ph.D., Takashi Matsukawa, M.D., and Hiroyuki Ishiura, M.D., Ph.D., Department of Neurology, Graduate School of Medicine, University of Tokyo, Tokyo; Yoko Fukuda, Ph.D., Department of Neurology, Graduate School of Medicine, University of Tokyo, Tokyo, and Max-Planck Institute of Immunobiology and Epigenetics, Freiburg, Germany; Yaeko Ichikawa, M.D., Ph.D., Hidetoshi Date, Ph.D., Budrul Ahsan, Ph.D., Yasuo Nakahara, M.D., Ph.D., Yoshio Momose, M.D., Ph.D., Yuji Takahashi, M.D., Ph.D., Atsushi Iwata, M.D., Ph.D., and Jun Goto, M.D., Ph.D., Department of Neurology, Graduate School of Medicine, University of Tokyo, Tokyo; Yorihiro Yamamoto, Ph.D., School of Bioscience and Biotechnology, Tokyo University of Technology, Tokyo; Makiko Komata, Ph.D., and Katsuhiko Shirahige, Ph.D., Center for Epigenetic Disease, Institute of Molecular and Cellular Biosciences, University of Tokyo, Tokyo; Kenju Hara, M.D., Ph.D., Department of Neurology, Brain Research Institute, Niigata University, Niigata, Japan; Akiyoshi Kakita, M.D., Ph.D., Mitsunori Yamada, M.D., Ph.D., and Hitoshi Takahashi, M.D., Ph.D., Department of Pathology, Brain Research Institute, Niigata University, Niigata, Japan; Osamu Onodera, M.D., Ph.D., and Masatoyo Nishizawa, M.D., Ph.D., Department of Neurology, Brain Research Institute, Niigata University, Niigata, Japan; Hiroshi Takashima, M.D., Ph.D., Department of Neurology and Geriatrics, Kagoshima University Graduate School of Medical and Dental Sciences, Kagoshima, Japan; Ryozo Kuwano, M.D., Ph.D., Department of Molecular Genetics, Center for Bioresources, Brain Research Institute, Niigata University, Niigata, Japan; Hirohisa Watanabe, M.D., Ph.D., Mizuki Ito, M.D., Ph.D., and Gen Sobue, M.D., Ph.D., Department of Neurology, Nagoya University Graduate School of Medicine, Nagoya, Japan; Hiroyuki Soma, M.D., Ph.D., Ichiro Yabe, M.D., Ph.D., and Hidenao Sasaki, M.D., Ph.D., Department of Neurology, Hokkaido University Graduate School of Medicine, Sapporo, Japan; Masashi Aoki, M.D., Ph.D., Department of Neurology, Tohoku University School of Medicine, Sendai, Japan; Kinya Ishikawa, M.D., Ph.D., and Hidehiro Mizusawa, M.D., Ph.D., Department of Neurology and Neurological Science, Graduate School of Medical and Dental Science, Tokyo Medical and Dental University, Tokyo; Kazuaki Kanai, M.D., Ph.D., Takamichi Hattori, M.D., Ph.D., and Satoshi Kuwabara, M.D., Ph.D., Department of Neurology, Chiba University School of Medicine, Chiba, Japan; Kimihito Arai, M.D., Ph.D., Division of Neurology, National Hospital Organization, Chiba East Hospital,

Chiba, Japan; Shigeru Koyano, M.D., Ph.D., Department of Clinical Neurology and Stroke Medicine, Graduate School of Medicine, Yokohama City University, Yokohama, Japan; Yoshiyuki Kuroiwa, M.D., Ph.D., Department of Neurology, Teikyo University School of Medicine University Hospital, Mizonokuchi, Kawasaki, Japan; Kazuko Hasegawa, M.D., Ph.D., Division of Neurology, National Hospital Organization, Sagamihara National Hospital, Sagamihara, Japan; Tatsuhiko Yuasa, M.D., Ph.D., Department of Neurology, Kamagaya-Chiba Medical Center for Intractable Neurological Disease, Kamagaya General Hospital, Chiba, Japan; Kenichi Yasui, M.D., Ph.D., and Kenji Nakashima, M.D., Ph.D., Division of Neurology, Department of Brain and Neurosciences, Faculty of Medicine, Tottori University, Yonago, Japan; Hijiri Ito, M.D., Ph.D., Department of Neurology, Mifukai Vihara Hananosato Hospital, Hiroshima, Japan; Yuishin Izumi, M.D., Ph.D., and Ryuji Kaji, M.D., Ph.D., Department of Clinical Neuroscience, Institute of Health Biosciences, University of Tokushima Graduate School, Tokushima, Japan; Takeo Kato, M.D., Ph.D., Departments of Neurology, Hematology, Metabolism, Endocrinology, and Diabetology, Faculty of Medicine, Yamagata University, Yamagata, Japan; Susumu Kusunoki, M.D., Ph.D., Department of Neurology, Kinki University School of Medicine, Osaka, Japan; Yasushi Osaki, M.D., Ph.D., Department of Geriatrics, Cardiology and Neurology, Kochi Medical School, Nankoku, Japan; Masahiro Horiuchi, M.D., Ph.D., Division of Neurology, Department of Internal Medicine, St. Marianna University School of Medicine, Kawasaki, Japan; Tomoyoshi Kondo, M.D., Ph.D., Department of Neurology, Wakayama Medical University, Wakayama, Japan; Shigeo Murayama, M.D., Ph.D., Department of Neuropathology and the Brain Bank for Aging Research, Tokyo Metropolitan Geriatric Hospital and Institute of Gerontology, Tokyo; Nobutaka Hattori, M.D., Ph.D., Department of Neurology, Juntendo University School of Medicine, Tokyo; Mitsutoshi Yamamoto, M.D., Ph.D., Department of Neurology, Kagawa Prefectural Central Hospital, Takamatsu, Japan; Miho Murata, M.D., Ph.D., Department of Neurology, National Center Hospital of Neurology and Psychiatry, Tokyo; Wataru Satake, M.D., Ph.D., and Tatsushi Toda, M.D., Ph.D., Division of Neurology/Molecular Brain Science, Kobe University Graduate School of Medicine, Kobe, Japan; Alexandra Dürr, M.D., Ph.D., and Alexis Brice, M.D., INSERM, UMR_S975, CRICM, F-75013, Paris, UPMC University of Paris 06, UMR_S975, F-75013, Paris, CNRS UMR 7225, F-75013, Paris, and Hôpital de la Salpêtrière, Département de Génétique et Cytogénétique, F-75013, Paris; Alessandro Filla, M.D., Department of Neurological Sciences, University Federico II, Naples, Italy; Thomas Klockgether, M.D., and Ullrich Wüllner, M.D., Ph.D., Department of Neurology, University of Bonn and German Center for Neurodegenerative Diseases (DZNE), Bonn, Germany; Garth Nicholson, M.B., B.S., Ph.D., University of Sydney at the Australian and New Zealand Army Corps (ANZAC) Research Institute, Concord Hospital, Sydney; Sid Gilman, M.D., Department of Neurology, University of Michigan, Ann Arbor; Clifford W. Shults, M.D.,* Department of Neurosciences, University of California, San Diego, School of Medicine, La Jolla; Caroline M. Tanner, M.D., Ph.D., Parkinson's Institute, Sunnyvale, CA; Walter A. Kukull, M.D., Department of Epidemiology, University of Washington School of Public Health, Seattle; Virginia M.-Y. Lee, Ph.D., Institute on Aging, Udall Parkinson's Research Center, Center for Neurodegenerative Disease Research and the Department of Pathology and Laboratory Medicine, Perelman School of Medicine at the University of Pennsylvania, Philadelphia; Eliezer Masliah, M.D., Department of Neurosciences, University of California San Diego, San Diego; Phillip A. Low, M.D., and Paola Sandroni, M.D., Ph.D., Department of Neurology, Mayo Clinic, Rochester, MN; John Q. Trojanowski, M.D., Ph.D., Institute on Aging, Udall Parkinson's Research Center, Center for Neurodegenerative Disease Research and the Department of Pathology and Laboratory Medicine, Perelman School of Medicine at the University of Pennsylvania, Philadelphia; Laurie Ozelius, Ph.D., Department of Genetics and Genomic Sciences, Mount Sinai School of Medicine, New York; Tatiana Foroud, Ph.D., Department of Medical and Molecular Genetics, Indiana University School of Medicine, Indiana Alcohol Research Center, Indianapolis; and Shoji Tsuji, M.D., Ph.D., Department of Neurology, Graduate School of Medicine and Medical Genome Center, University of Tokyo, Tokyo.

*Deceased.

REFERENCES

1. Graham JG, Oppenheimer DR. Orthostatic hypotension and nicotine sensitivity in a case of multiple system atrophy. J Neurol Neurosurg Psychiatry 1969;32:28-34.
2. Tu PH, Galvin JE, Baba M, et al. Glial cytoplasmic inclusions in white matter oligodendrocytes of multiple system atrophy brains contain insoluble alpha-synuclein. Ann Neurol 1998;44:415-22.
3. Wakabayashi K, Yoshimoto M, Tsuji S, Takahashi H. Alpha-synuclein immunoreactivity in glial cytoplasmic inclusions in multiple system atrophy. Neurosci Lett 1998;249:180-2.
4. Arima K, Uéda K, Sunohara N, et al. NACP/alpha-synuclein immunoreactivity in fibrillary components of neuronal and oligodendroglial cytoplasmic inclusions in the pontine nuclei in multiple system atrophy. Acta Neuropathol 1998;96:439-44.
5. Spillantini MG, Crowther RA, Jakes R, Cairns NJ, Lantos PL, Goedert M. Filamentous alpha-synuclein inclusions link multiple system atrophy with Parkinson's disease and dementia with Lewy bodies. Neurosci Lett 1998;251:205-8.
6. Papp MI, Kahn JE, Lantos PL. Glial cytoplasmic inclusions in the CNS of patients with multiple system atrophy (striatonigral degeneration, olivopontocerebellar atrophy and Shy-Drager syndrome). J Neurol Sci 1989;94:79-100.
7. Nakazato Y, Yamazaki H, Hirato J, Ishida Y, Yamaguchi H. Oligodendroglial microtubular tangles in olivopontocerebellar atrophy. J Neuropathol Exp Neurol 1990;49:521-30.
8. Gilman S, Wenning GK, Low PA, et al. Second consensus statement on the diagnosis of multiple system atrophy. Neurology 2008;71:670-6.
9. Watanabe H, Saito Y, Terao S, et al. Progression and prognosis in multiple system atrophy: an analysis of 230 Japanese patients. Brain 2002;125:1070-83.
10. Tsuji S, Onodera O, Goto J, Nishizawa M. Sporadic ataxias in Japan — a population-based epidemiological study. Cerebellum 2008;7:189-97.
11. Geser F, Seppi K, Stampfer-Kountchev M. The European Multiple System Atrophy-Study Group (EMSA-SG). J Neural Transm 2005;112:1677-86.
12. May S, Gilman S, Sowell BB, et al. Potential outcome measures and trial design issues for multiple system atrophy. Mov Disord 2007;22:2371-7.
13. Hara K, Momose Y, Tokiguchi S, et al. Multiplex families with multiple system atrophy. Arch Neurol 2007;64:545-51.
14. Wüllner U, Schmitt I, Kammal M, Kretzschmar HA, Neumann M. Definite multiple system atrophy in a German family. J Neurol Neurosurg Psychiatry 2009;80:449-50.
15. Hohler AD, Singh VJ. Probable hereditary multiple system atrophy-autonomic (MSA-A) in a family in the United States. J Clin Neurosci 2012;19:479-80.
16. Fukuda Y, Nakahara Y, Date H, et al. SNP HiTLink: a high-throughput linkage analysis system employing dense SNP data. BMC Bioinformatics 2009;10:121.
17. Gudbjartsson DF, Thorvaldsson T, Kong A, Gunnarsson G, Ingolfsdottir A. Allegro version 2. Nat Genet 2005;37:1015-6.
18. Li H, Durbin R. Fast and accurate short read alignment with Burrows-Wheeler transform. Bioinformatics 2009;25:1754-60.
19. Li H, Handsaker B, Wysoker A, et al. The Sequence Alignment/Map format and SAMtools. Bioinformatics 2009;25:2078-9.
20. Burón MI, Hermán MD, Alcaín FJ, Villalba JM. Stimulation of polyprenyl

4-hydroxybenzoate transferase activity by sodium cholate and 3-[(cholamidopropyl) dimethylammonio]-1-propanesulfonate. Anal Biochem 2006;353:15-21.
21. Yamashita S, Yamamoto Y. Simultaneous detection of ubiquinol and ubiquinone in human plasma as a marker of oxidative stress. Anal Biochem 1997;250: 66-73.
22. Blin O, Desnuelle C, Rascol O, et al. Mitochondrial respiratory failure in skeletal muscle from patients with Parkinson's disease and multiple system atrophy. J Neurol Sci 1994;125:95-101.
23. Martinelli P, Giuliani S, Lodi R, Iotti S, Zaniol P, Barbiroli B. Failure of brain and skeletal muscle energy metabolism in multiple system atrophy shown by in vivo phosphorous MR spectroscopy. Adv Neurol 1996;69:271-7.
24. Yamashita T, Ando Y, Obayashi K, et al. Oxidative injury is present in Purkinje cells in patients with olivopontocerebellar atrophy. J Neurol Sci 2000;175:107-10.
25. Stefanova N, Reindl M, Neumann M, et al. Oxidative stress in transgenic mice with oligodendroglial alpha-synuclein overexpression replicates the characteristic neuropathology of multiple system atrophy. Am J Pathol 2005;166:869-76.
26. Stefanova N, Georgievska B, Eriksson H, Poewe W, Wenning GK. Myeloperoxidase inhibition ameliorates multiple system atrophy-like degeneration in a transgenic mouse model. Neurotox Res 2012; 21:393-404.
27. Ubhi K, Lee PH, Adame A, et al. Mitochondrial inhibitor 3-nitroproprionic acid enhances oxidative modification of alpha-synuclein in a transgenic mouse model of multiple system atrophy. J Neurosci Res 2009;87:2728-39.
28. Ubhi K, Rockenstein E, Mante M, et al. Alpha-synuclein deficient mice are resistant to toxin-induced multiple system atrophy. Neuroreport 2010;21:457-62.
29. López-Martín JM, Salviati L, Trevisson E, et al. Missense mutation of the COQ2 gene causes defects of bioenergetics and de novo pyrimidine synthesis. Hum Mol Genet 2007;16:1091-7.
30. Diomedi-Camassei F, Di Giandomenico S, Santorelli FM, et al. COQ2 nephropathy: a newly described inherited mitochondriopathy with primary renal involvement. J Am Soc Nephrol 2007;18:2773-80.
31. Sasaki H, Emi M, Iijima H, et al. Copy number loss of (src homology 2 domain containing)-transforming protein 2 (SHC2) gene: discordant loss in monozygotic twins and frequent loss in patients with multiple system atrophy. Mol Brain 2011; 4:24.
32. Al-Chalabi A, Dürr A, Wood NW, et al. Genetic variants of the alpha-synuclein gene SNCA are associated with multiple system atrophy. PLoS One 2009;4(9): e7114.
33. Scholz SW, Houlden H, Schulte C, et al. SNCA variants are associated with increased risk for multiple system atrophy. Ann Neurol 2009;65:610-4. [Erratum, Ann Neurol 2010;67:277.]
34. Tsuji S. Genetics of neurodegenerative diseases: insights from high-throughput resequencing. Hum Mol Genet 2010;19: R65-R70.
35. Ferrante KL, Shefner J, Zhang H, et al. Tolerance of high-dose (3,000 mg/day) coenzyme Q10 in ALS. Neurology 2005; 65:1834-6.
36. Hyson HC, Kieburtz K, Shoulson I, et al. Safety and tolerability of high-dosage coenzyme Q10 in Huntington's disease and healthy subjects. Mov Disord 2010; 25:1924-8.

Journal of Human Genetics (2013) 58, 711–719

www.nature.com/jhg

ORIGINAL ARTICLE

YY1 binds to α-*synuclein* 3′-flanking region SNP and stimulates antisense noncoding RNA expression

Ikuko Mizuta[1,2], Kazuaki Takafuji[3], Yuko Ando[1], Wataru Satake[1], Motoi Kanagawa[1], Kazuhiro Kobayashi[1], Shushi Nagamori[3], Takayuki Shinohara[1], Chiyomi Ito[1], Mitsutoshi Yamamoto[4], Nobutaka Hattori[5], Miho Murata[6], Yoshikatsu Kanai[3], Shigeo Murayama[7], Masanori Nakagawa[8] and Tatsushi Toda[1]

α-*synuclein* (*SNCA*) is an established susceptibility gene for Parkinson's disease (PD), one of the most common human neurodegenerative disorders. Increased SNCA is considered to lead to PD and dementia with Lewy bodies. Four single-nucleotide polymorphisms (SNPs) in *SNCA* 3′ region were prominently associated with PD among different ethnic groups. To examine how these SNPs influence disease susceptibility, we analyzed their potential effects on *SNCA* gene expression. We found that rs356219 showed allele-specific features. Gel shift assay using nuclear extracts from SH-SY5Y cells showed binding of one or more proteins to the protective allele, rs356219-A. We purified the rs356219-A–protein complex with DNA affinity beads and identified a bound protein using mass spectrometry. This protein, YY1 (Yin Yang 1), is an ubiquitous transcription factor with multiple functions. We next investigated *SNCA* expression change in SH-SY5Y cells by YY1 transfection. We also analyzed the expression of antisense noncoding RNA (ncRNA) *RP11-115D19.1* in *SNCA* 3′-flanking region, because rs356219 is located in intron of *RP11-115D19.1*. Little change was observed in *SNCA* expression levels; however, *RP11-115D19.1* expression was prominently stimulated by YY1. In autopsied cortices, positive correlation was observed among *RP11-115D19.1*, *SNCA* and *YY1* expression levels, suggesting their functional interactions *in vivo*. Knockdown of *RP11-115D19.1* increased *SNCA* expression significantly in SH-SY5Y cells, suggesting its repressive effect on *SNCA* expression. Our findings of the protective allele-specific YY1 and antisense ncRNA raised a novel possible mechanism to regulate *SNCA* expression.
Journal of Human Genetics (2013) **58,** 711–719; doi:10.1038/jhg.2013.90; published online 12 September 2013

Keywords: α-*synuclein*; association; ncRNA; Parkinson's disease susceptibility; SNP; YY1

INTRODUCTION

Parkinson's disease (PD) (OMIM 168600) is one of the most common human neurodegenerative disorders, affecting 1–2% of people aged ⩾65 years.[1] Clinical features of PD (parkinsonism) include resting tremor, bradykinesia, rigidity and postural instability. PD is characterized pathologically by the loss of dopaminergic neurons in the substantia nigra of the midbrain and by the presence of intracellular inclusions known as Lewy bodies.[2]

Linkage studies for Mendelian-inherited PD have identified autosomal dominant genes, including α-*synuclein* (*SNCA*) and *LRRK2*, as well as the autosomal recessive genes *parkin*, *PINK1*, *DJ-1*, *ATP13A2*, *PLA2G6* and *FBXO7*.[3,4] However, Mendelian-inherited PD is rare compared with the far more common sporadic PD, a complex disorder caused by multiple genetic and environmental factors.[5]

SNCA was the first-identified causal gene for Mendelian-inherited PD.[6] The missense mutation A53T was identified in the original autosomal-dominant family, followed by confirmation of SNCA protein as a major component of Lewy bodies, the pathological hallmark of PD in both Mendelian-inherited and sporadic cases.[6,7] To date, three missense mutations and multiplication of *SNCA* have been identified in familial PD. Missense mutations are thought to increase the aggregation of SNCA protein. In patients with triplication of the *SNCA* locus, a doubling of wild-type *SNCA* gene dosage by triplication has been shown to result in the doubling of mRNA and protein expression in blood and in the brain.[8,9] Duplication of *SNCA* has also been implicated in familial PD. Patients with *SNCA* duplications show much milder clinical features than do those with *SNCA* triplications, more closely resembling sporadic cases.[10,11]

SNCA is also a causal gene for Mendelian-inherited dementia with Lewy bodies (DLB) (OMIM 127750). DLB, usually sporadic, is characterized clinically by dementia and parkinsonism and

[1]Division of Neurology/Molecular Brain Science, Kobe University Graduate School of Medicine, Kobe, Japan; [2]Department of Neurology, Graduate School of Medical Science, Kyoto Prefectural University of Medicine, Kyoto, Japan; [3]Division of Bio-system Pharmacology, Department of Pharmacology, Graduate School of Medicine, Osaka University, Suita, Japan; [4]Department of Neurology, Kagawa Prefectural Central Hospital, Takamatsu, Japan; [5]Department of Neurology, Juntendo University School of Medicine, Tokyo, Japan; [6]Department of Neurology, National Center Hospital, National Center of Neurology and Psychiatry, Kodaira, Japan; [7]Department of Neuropathology, Tokyo Metropolitan Institute of Gerontology, Tokyo, Japan and [8]North Medical Center, Kyoto Prefectural University of Medicine, Kyoto, Japan
Correspondence: Professor T Toda, Division of Neurology/Molecular Brain Science, Kobe University Graduate School of Medicine, 7-5-1 Kusunoki-chou, Chuo-ku, Kobe 650-0017, Japan.
E-mail: toda@med.kobe-u.ac.jp
Received 24 April 2013; revised 31 July 2013; accepted 2 August 2013; published online 12 September 2013

pathologically by widespread Lewy bodies. According to the overlapped features, PD and DLB are collectively called Lewy body diseases (LBD).

A popular hypothesis is that SNCA aggregation has a crucial role in neuronal loss and Lewy body formation and that increased SNCA leads to LBD. In this scenario, PD-associated *SNCA* polymorphisms might influence *SNCA* expression levels in sporadic PD. We and the others have previously reported that single-nucleotide polymorphisms (SNPs) in the *SNCA* 3′region were prominently associated with sporadic PD in both the Japanese and European populations.[12,13] Moreover, our recent genome-wide association study (GWAS) in the Japanese population,[14] as well as a GWAS analysis in individuals of European ancestry,[15] confirmed a strong association with the *SNCA* 3′region. In this report, we have examined how *SNCA* SNPs might influence LBD susceptibility.

MATERIALS AND METHODS

Genotyping

As described previously,[13] we recruited 882 unrelated sporadic PD patients (age: 64.9 ± 9.8 years; male/female ratio: 0.79) and 938 unrelated controls (age: 45.3 ± 16.3 years; male/female ratio: 1.10). The diagnosis of idiopathic PD was based on the presence of ⩾2 of the cardinal features of PD (tremor, rigidity, bradykinesia and postural instability), according to the criteria for sporadic PD.[16] Patients were evaluated by certified neurologists specializing in PD. The average age of onset was 57.4 ± 10.9 years. Forty-two patients showed early onset of PD (<40 years of age), and 51 patients had a positive family history of PD. Patients who carried *parkin* mutations were excluded. All patients and controls were of Japanese ancestry. Informed consent was obtained from each individual, and approval for the study was obtained from the University Ethical Committees. Genomic DNA was extracted from the whole blood using FlexGene (Qiagen GmbH, Hilden, Germany). The rs356219, rs356220 and rs356203 SNPs were genotyped using TaqMan (Applied Biosystems, Lifetechnologies Corp., Carlsbad, CA, USA). SNPAlyze software (DYNACOM, Chiba, Japan) was used for pairwise linkage disequilibrium analysis (Lewontin's coefficient, D′, and standardized coefficient, *r*).

Luciferase assay

DNA fragments of ~250 bp corresponding to the regions containing four *SNCA* SNPs (rs356219, rs356220, rs356165 and rs356203) were amplified by PCR using heterozygous genomic DNA as template and then cloned into the SalI site of the pGL3-promoter vector (Promega Corporation, Madison, WI, USA). The orientation and allele identity of the insert were determined by DNA sequence analysis. Primer sequences used for PCR are listed in Supplementary Table 1. The human neuroblastoma cell line SH-SY5Y was grown in Dulbecco's Modified Eagle's medium supplemented with 10% fetal bovine serum and antibiotics. We transfected cells (3×10^5 cells per well on 24-well plates) with 360 ng of each construct and 40 ng of pRL-TK vector (Promega), as an internal control for transfection efficiency, using Effectene (Qiagen). After 48 h, cells were solubilized, and luciferase activity was measured using the dual luciferase assay system (Promega).

Preparation of nuclear extract

Nuclear extracts from SH-SY5Y cells were prepared as previously described, with minor modifications.[17] In brief, cells were washed and re-suspended in buffer A (10 mM 4-(2-hydroxyethyl)-1-piperazineethanesulfonic acid (HEPES)-KOH pH7.8, 10 mM KCl, 0.1 mM EDTA pH8.0, 0.1% NP-40, 1 mM dithiothreitol (DTT) and protease inhibitor cocktail (NACALAI TESQUE, Inc., Kyoto, Japan)). Nuclei were pelleted and re-suspended in buffer C (50 mM HEPES-KOH pH7.8, 420 mM KCl, 0.1 mM EDTA pH8.0, 5 mM $MgCl_2$, 2% glycerol, 1 mM DTT and protease inhibitor cocktail). After vortexing every 5 min for 30 min on ice, the samples were centrifuged, and the supernatants were used as nuclear extract.

Gel shift assay

Gel shift assays were performed as previously described.[18] SH-SY5Y nuclear extract (5–10 μg protein) was incubated with 0.031 pmol of 33-bp oligonucleotides (Supplementary Table 2) labeled with digoxigenin-11-ddUTP in 20 μl of binding buffer (20 mM HEPES pH7.6, 1 mM EDTA, 10 mM $(NH_4)_2SO_4$, 1 mM DTT, 0.2% Tween 20 and 30 mM KCl) containing 1 μg of poly(dI-dC) for 20 min, using the DIG gel shift kit (Roche Diagnostics, Mannheim, Germany). For competition studies, nuclear extract was pre-incubated with 3.85 pmol of unlabeled oligonucleotide before addition of the labeled probe. Supershift assays were performed by incubating the protein–DNA complexes with 0.8 μg of rabbit immunoglobulin G or rabbit polyclonal anti-YY1 (anti-Yin Yang 1; Active Motif, Carlsbad, CA, USA) for 5 min. The protein–DNA complexes were separated on DNA retardation polyacrylamide gels (Invitrogen, Lifetechnologies Corp., Carlsbad, CA, USA) and transferred to Hybond-N + Nylon membrane (GE Healthcare, Amersham Place, UK). All assays and gel electrophoresis procedures were performed at 4 °C. Signal detection was performed using the CSPD chemiluminescent detection system (Roche Diagnostics).

Ultraviolet (UV) cross-linking

The size of the rs356219-A binding protein was determined by UV cross-linking. We incubated 0.05 pmol of ^{32}P-labeled 33 bp rs356219-A oligonucleotide with SH-SY5Y nuclear extract and 6.16 pmol of unlabeled 33 bp competitor (rs356219-G or -A) for 15 min at 4 °C in the solution used for the gel shift assays. DNA–protein complexes were transferred to a flat-bottom 96-well plate, placed on a transilluminator and irradiated (312 nm, 15 min at 4 °C). Samples were run on 10% NuPAGE Novex Bis-Tris gels (Invitrogen), dried and autoradiographed.

Purification of the rs356219-A binding protein using affinity magnetic beads

Oligonucleotides containing rs356219-A with 5′-TCGA-3′ linkers were ligated in a head-to-tail manner and inserted into the SalI site of the pGL3-promoter vector (Promega). A fragment with 14 tandem repeats of rs356219-A was amplified from the plasmid by PCR using a biotin-labeled forward primer (5′-GGTAAAATCGATAAGGATCC-3′) and a non-labeled reverse primer (5′-TT GAAGGCTCTCAAGGGCAT-3′). The biotinylated PCR product (30 pmol) was bound to 1 mg of Dynabeads M-280 streptavidin (Dynal, Life Technologies, Carlsbad, CA, USA). Fifty microliters of SH-SY5Y nuclear extract, prepared with Buffer C containing 200 mM KCl, was precleared in 1 ml of binding buffer in the presence of 1 mg of unbound beads and 144 pmol of 33 bp non-labeled competitor rs356219-A or -G. Following magnetic separation, the supernatant was incubated with 1 mg of probe-bound Dynabeads for 30 min at 4°C. The beads were washed five times and then eluted sequentially, twice with 40 μl elution buffer (20 mM HEPES-KOH pH7.6, 1 mM EDTA, 10 mM $(NH_4)_2SO_4$, 1 mM DTT, 0.2% Tween 20, protease inhibitor cocktail and 10% glycerol) containing 200 mM KCl and twice with 40 μl elution buffer containing 300 mM KCl. Proteins in each elute were analyzed by electrophoresis on 10% NuPAGE Novex Bis-Tris gel (Invitrogen). Binding activity of each elute was evaluated by gel shift assay.

In-gel digestion

Protein bands were excised from a silver-stained gel. Proteins were digested with sequencing grade-modified trypsin (Roche Diagnostics) as described elsewhere.[19] Tryptic peptides were extracted from gel pieces in 50% acetonitrile with 5% formic acid and dried using a vacuum centrifuge. Dried peptides were resuspended in 5% acetonitrile containing 0.1% trifluoroacetic acid and desalted using StageTips with a C18 Empore disk membrane (3M, Minneapolis, MN, USA) according to the published procedure.[20]

Liquid chromatography-tandem mass spectrometry (LC-MS/MS) and data analysis

LC-MS/MS analysis was performed using a Paradigm MS4 nanoHPLC system (Michrom BioResources, Inc., Auburn, CA, USA) coupled to a LTQ linear ion trap mass spectrometer (Thermo Electron Corp., Waltham, MA, USA) with a

nanoelectrospray ionization source (AMR Inc., Tokyo, Japan). Tryptic peptides were injected by a HTC-PAL autosampler (CTC Analytics, Zwingen, Switzerland) and enriched on a C18 trap column (300 μm I.D. × 5 mm length, CERI, Tokyo, Japan) at a flow rate of 6 μl min^{-1}. The samples were subsequently separated by a C18 reverse phase column (100 μm I.D. × 150 mm length, Nikkyo Technos, Tokyo, Japan) at a flow rate of 1 μl min^{-1}, with a linear gradient from 2% to 65% mobile phase B, that is; from 98% to 35% of mobile phase A. The mobile phase B consisted of 95% acetonitrile with 0.1% formic acid, whereas the mobile phase A consisted of 2% acetonitrile with 0.1% formic acid. LC-MS/MS analysis was carried out using a data-dependent triple-play mode. Automated gain control values were set at 1.5×10^4, 1.5×10^3 and 5.0×10^3 for Full-MS, Zoom-MS and MS/MS, respectively. A spray voltage of 2.4 kV was applied. The MS scan range was *m/z* 300–2000. Peptides and proteins were identified by Mascot software ver. 2.2 (Matrix Science, London, UK), screened against the most recent version of the human IPI database from EMBL-EBI (http://www.ebi.ac.uk/IPI/IPIhuman.html). Maximum tolerance was set to 1.2 Da for MS data, 0.5 Da for MS/MS data and strict trypsin specificity allowing for up to one missed cleavage. Carbamidomethylation of cysteine and oxidation of methionine were allowed as variable modifications.

Transfection of YY1

SH-SY5Y cells were transfected with pCMV6-XL5 expressing human YY1 (OriGene, Rockville, MD, USA) or blank vector by using an electroporator CUY21 *Pro-Vitro* (NEPA GENE, Chiba, Japan). Twenty-four hours after transfection, the cells were harvested. For western blotting, whole-cell lysates were separated by electrophoresis on 10% NuPAGE Novex Bis-Tris gel and blotted onto PVDF membrane (Immobilon-P, Merck Millipore, Darmstadt, Germany). The membranes were incubated with anti-YY1 (sc-1703, Santa Cruz Biotechnology, Santa Cruz, CA, USA) or anti-Actin (sc-10731, Santa Cruz Biotechnology), followed by reaction with horseradish peroxidase-conjugated secondary antibodies. Signal detection was performed using the ECL detection system (Thermo Fisher Scientific, Rockford, IL, USA).

Overexpression/knockdown of *RP11-115D19.1*

For overexpression experiment, *RP11-115D19.1-003* cDNA (469 bp) was amplified from SH-SY5Y cDNA and *RP11-115D19.1-005* cDNA (567 bp) was synthesized (Genscript, Piscataway, NJ, USA). Each fragment was cloned into pCMV6-XL5 and transfected to SH-SY5Y cells as described above. For repression experiment, siRNA targeting to *RP11-115D19.1* (5′-CATGCTTC-CAGAGAATGCATATTCT-3′) was designed from the common region between *RP11-115D19.1-003* and *-005*. The siRNA and negative control (Lo GC duplex) were purchased (Stealth RNAi, Invitrogen) and transfected as described above. Twenty-four hours after transfection, the cells were harvested.

Real-time reverse transcription-PCR (RT-PCR)

As described previously, autopsied frontal cortices were obtained from the Brain Bank for Aging Research (Tokyo Metropolitan Geriatric Hospital/Tokyo Metropolitan Institute of Gerontology) and Department of Neurology, Juntendo University School of Medicine, Tokyo, Japan. The samples contained 21 cases (age, 82.6 ± 7.1 (s.d.) years; 11 males and 10 females) with Lewy body pathology defined by the third Consensus Guideline for Dementia with Lewy Bodies, comprising PD with and without dementia and DLB and 18 control subjects (age, 81.2 ± 5.2 years; 12 males and 6 females) without parkinsonism or dementia and without neurodegenerative pathological changes. Total RNA was extracted from SH-SY5Y cells or tissue using RNeasy (Qiagen), and cDNA was prepared using High Capacity RNA-to-cDNA kit (Applied Biosystems). Real-time RT-PCR was carried out on StepOnePlus real-time PCR system (Applied Biosystems) using Fast SYBR Green Master Mix (Applied Biosystems). First-strand cDNA was amplified using primers specific for *SNCA* (forward; 5′-CAGAAGCAGCAGGAAAGACA-3′, reverse; 5′-CCACTGCTCCT CCAACATTT-3′, product size; 132 bp), *RP11-115D19.1-003* (forward; 5′-TAA AACCTGCAAATTCACATCTTC-3′, reverse; 5′-AAGTAGGTAAGTAGGGCAG TGCAT-3′ product size; 133 bp), *RP11-115D19.1-005* (forward; 5′-CCATGCTT CCAGAGAATGCA-3′, reverse; 5′-GTGCTTCCCTTTCACTGAAG-3′, product size; 144 bp), *GAPDH* (forward; 5′-CATCTTCCAGGAGCGAGATC-3′, reverse; 5′-TGCAAATGAGCCCCAGCCTT-3′, product size; 114 bp), *NF* (*neurofilament L*, forward; 5′-AAGAACACCGACGCCGTGCG-3′, reverse; 5′-TGCCATTTCACTCTTTGTGG-3′, product size; 222 bp), and *YY1* (forward; 5′-TGGCAAAGCTTTTGTTGAGA-3′, reverse; 5′-ATGTGTGCGCAAATTGA AGT-3′, product size; 130 bp). For quantification, we used a relative standard curve method and amplified cDNA corresponding to 100 ng (*RP11-115D19.1*) or 1.7 ng (*SNCA*, *GAPDH*, and *NF*) RNA per well. Standard curves were generated from amplification of diluted series of cDNA from cortices (*SNCA*, *GAPDH*, and *NF*), YY1-transfected SH-SY5Y cells (*RP11-115D19.1*) or plasmids (pCMV-YY1, pCMV-RP11-115D19.1-003, pCMV-RP11-115D19.1-005). *SNCA*, *RP11-115D19.1* and *YY1* expression levels were normalized to those of *GAPDH* (SH-SY5Y cells) or *NF* (cortices). The values were determined in triplicate or duplicate. Genotyping of rs356219 of SH-SY5Y and cortices was performed using restriction fragment length polymorphism and sequencing.

RESULTS

Identification of four *SNCA* SNPs associated with PD in both the Japanese and European populations

We previously identified six SNPs (rs3857053, rs356165, rs7684318, rs3775424, rs3796661 and rs2737029), located in the 3′-flanking, 3′-UTR and intron 4 of *SNCA*, that were prominently associated with PD.[13] Independently, analysis of a European population also reported

Table 1 PD-associated *SNCA* SNPs reported in the Japanese and German studies

	Position	Region	Japanese study[a]		German study[b]		MAF of Europeans in the dbSNP database		
SNP ID	(NCBI build 36)		P-value	MAF (Case/control)	P-value	MAF (Case/control)	HapMap-CEU	EGP_CEPH_PANEL	AFD_EUR_PANEL
rs356219	90637601	3′-Flanking	7.3×10^{-9}	0.34/0.43	0.00467	0.46/0.38	0.425		0.354
rs356220	90641340	3′-Flanking	8.7×10^{-10}	0.33/0.43	0.00485	0.46/0.38	0.427		
rs3857053	90645674	3′-Flanking	1.1×10^{-9}	0.33/0.43				0.071	
rs356165	90646886	3′-UTR	2.0×10^{-9}	0.33/0.43	0.00555	0.46/0.38	0.433	0.412	
rs7684318	90655003	Intron 4	5.0×10^{-10}	0.33/0.43					0.024
rs3775424	90665256	Intron 4	5.4×10^{-10}	0.33/0.43			0.033		
rs356203	90666041	Intron 4	1.4×10^{-7}	0.34/0.43	0.00548	0.46/0.38		0.45	
rs3796661	90687507	Intron 4	2.7×10^{-9}	0.33/0.42			0.033		0.021
rs2737029	90711770	Intron 4	1.7×10^{-11}	0.32/0.42	0.09994	0.46/0.42	0.45		0.396

Abbreviations: MAF, minor allele frequency; NCBI, National Center for Biotechnology Information; PD, Parkinson's disease; *SNCA*, α-*synuclein*; SNP, single-nucleotide polymorphism; UTR, untranslated region.
[a]From our previous study[13] and present study (rs356219, rs356220 and rs356203).
[b]From the previous German study[12] (replication sample set II).

strong association for four SNPs (rs356219, rs356220 rs356165, rs356203) in the 3′-flanking region of *SNCA*.[12] Of these SNPs, only rs356165 was common to the two studies. We genotyped the remaining SNPs of the European population (rs356219, rs356220 and rs356203) and confirmed their prominent association with the Japanese population (Table 1, Figure 1a). The remaining SNPs reported in the Japanese population study were rare in the European population (Table 1, Figure 1a). From these findings, we concluded that rs356219, rs356220, rs356165 and rs356203 were associated prominently with PD in both the populations. Our functional analysis focused on these four SNPs.

Allele-specific effect of rs356219 in luciferase and gel shift assays

To determine whether the four SNPs could affect *SNCA* expression levels, we constructed plasmids containing genomic fragments with each SNP, placed downstream from a luciferase transcriptional unit (Figure 1b). For rs356219, the clone containing the protective A allele showed 1.6-fold greater luciferase activity than did the disease-associated G allele. We observed no allele-specific differences for the remaining three SNPs, however. Next, we used gel shift assays to examine the possibility that proteins might bind to the SNPs in an allele-specific manner (Figure 1c). The protective rs356219-A allele showed an intense shift band relative to the disease allele rs356219-G. Alleles of rs356220 and rs356165 showed similar shift band intensities. For rs356203, the intensity of the C disease allele was stronger than that of the protective T allele. We focused our subsequent analyses on rs356219, which was the only SNP that showed allele-specific features in both the assays.

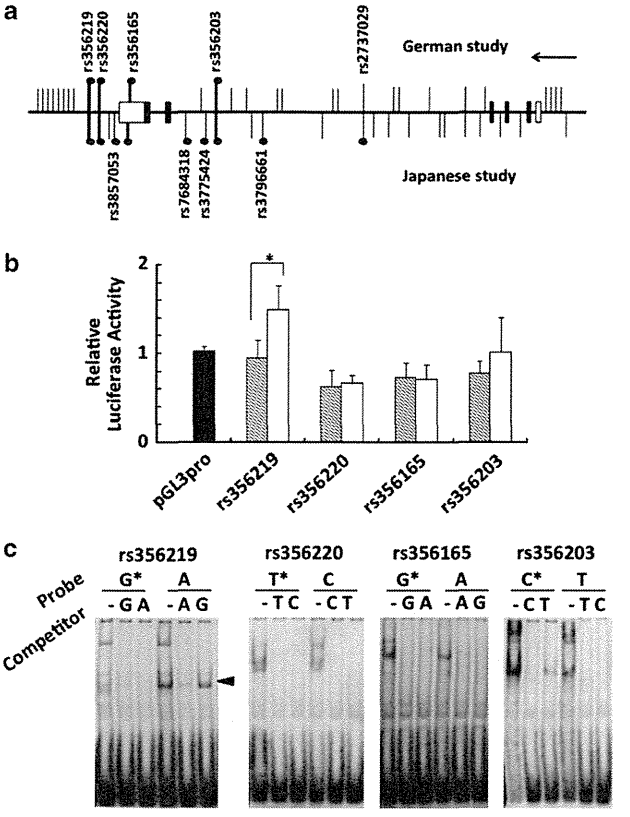

Figure 1 Transcriptional regulatory activity affected by *SNCA* SNPs. (**a**) Schematic representation of the *SNCA* gene with relative positions of SNPs genotyped in the Japanese and European population studies. The *SNCA* locus (horizontal line), coding regions (black boxes), 5′- and 3′-UTR (white boxes) and transcription orientation (arrow) are shown. The relative positions of SNPs (vertical lines) genotyped in the Japanese study (lower) and the German study (upper) are represented. Of the SNPs strongly associated with each study (solid circle), four SNPs are commonly associated with PD in both the studies (thick vertical lines). (**b**) Luciferase assay. Luciferase activities relative to the control pGL3-promoter construct (black bar) were compared between disease allele (shaded) and protective allele (white) at each of the four SNPs ($n=7$). Luciferase activity of the protective rs356219-A allele was significantly increased relative to that of the G disease allele (*$P=0.001$ by Student's *t*-test). (**c**) Gel shift assay. Binding of SH-SY5Y nuclear protein to alleles at the four SNPs are presented. Shift bands were compared between the disease allele (*) and the protective allele at each SNP. The intense shift band observed for the protective allele rs356219-A was competed by non-labeled competitor allele A but not by the disease allele G (arrowhead).

Identification of the rs356219-A binding protein

We performed UV-crosslinking and estimated the size of the protein bound to the rs356219-A allele at ~55 kDa (Figure 2a). Next, we purified the protein by binding to rs356219-A affinity beads in the presence of non-biotinylated rs356219-G fragments as a competitor. Control experiments used non-biotinylated rs356219-A fragments as competitor. After washing, the binding protein was eluted sequentially, twice with elution buffer containing 200 mM KCl and twice with buffer containing 300 mM KCl. Electrophoresis and gel shift assay located the ~55 kDa band and binding activity within the second (200 mM KCl) and third (300 mM KCl) elutes. Both were absorbed by the rs356219-A competitor in the control experiments (Figure 2b). Subsequent LC-MS/MS analysis showed that peptides derived from a transcription factor YY1 were identified from the ~55 kDa bands (Figure 2c). We concluded that the rs356219-A binding protein was YY1. This observation was confirmed by super-shift assays using anti-YY1 antibody (Figure 2d, Supplementary Figure 1).

Effects of YY1 transfection on *SNCA* and noncoding RNA (ncRNA) *RP11-115D19.1* expression in SH-SY5Y cells

Luciferase assay and gel shift assay suggested that YY1 bound to rs356219 protective allele and stimulated transcription (Figures 1b and c and 2). Recent Ensemble Genome Browser showed antisense ncRNA named *RP11-115D19.1* in *SNCA* 3′-flanking region. The SNP rs356219 locates intron of its two spliced isoforms (*RP11-115D19.1-003* and *-005*; Figure 3a), suggesting that rs356219 might influence transcription of *SNCA* and/or *RP11-115D19.1*. If rs356219 influences *SNCA* promoter, increased luciferase activity in the protective allele (Figure 1b) appears incompatible with the hypothesis that increased SNCA leads to PD. To address this issue, we investigated YY1-induced expression of *SNCA* and *RP11-115D19.1* in SH-SY5Y neuroblastoma cells, whose genotype of rs356219 was heterozygous. YY1 transfection showed 23-fold increase in *RP11-115D19.1-003*, 24-fold increase in *RP11-115D19.1-005* and twofold increase in *SNCA* expression levels (Figure 3b). Other two independent transfection experiments replicated the prominent stimulation of *RP11-115D19.1* by YY1; however, they showed little changes of *SNCA* expression (data not shown). We analyzed allele-specific expression level of *SNCA* by using 3′-UTR SNP rs356165 as a marker and found little difference between the alleles, both in YY1 and blank transfection (Figure 3c). We could not analyze allele-specific expression of *RP11-115D19.1*, because no SNP was found in *RP11-115D19.1* exons in SH-SY5Y. Although the role of *RP11-115D19.1* on *SNCA* expression remains uncovered, increased luciferase activity in the

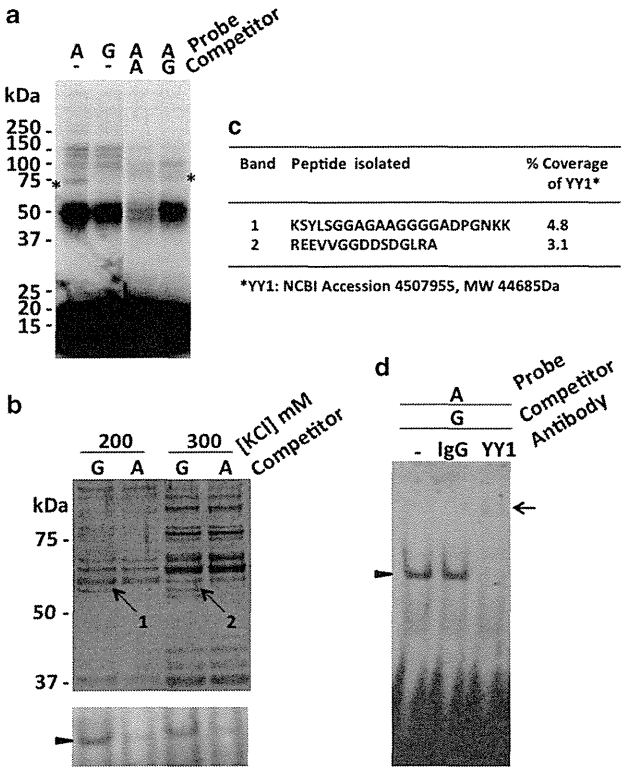

Figure 2 Purification and identification of the rs356219-A binding protein. (**a**) Estimation of the molecular size of the rs356219-A binding protein by UV cross-linking analysis. SH-SY5Y nuclear extract was incubated with the probe, rs356219-A (protective allele) or rs356219-G (disease allele) in the presence or absence of non-labeled competitor. Following UV irradiation, the cross-linked protein–probe complexes were analyzed by SDS-PAGE. The size of allele A and protein complex was estimated as ~70 kDa (*). As the mean size of the free probe was estimated as ~15 kDa, the protein of interest was estimated as ~55 kDa. (**b**) Purification of the rs356219-A binding protein using DNA affinity beads. Nuclear extract from SH-SY5Y cells was incubated with affinity beads bound to tandem repeats of 33 bp region containing the A allele, in the presence of free competitor G allele (for purification) or control allele A. After the binding reaction, beads were washed and eluted twice with buffer containing 200 mM KCl and then twice with buffer containing 300 mM KCl. Aliquots of each elution were analyzed by SDS-PAGE (upper panel) and gel shift assays using rs356219-A as a probe (lower panel). The second and third elutions are shown. The rs356219-A binding band of ~55 kDa was observed (bands 1 and 2, arrows) and correlated with the intensity of the gel shift band (arrowhead). (**c**) Summary of mass spectrometry analysis of the two ~55 kDa bands. Peptides derived from YY1 were identified from both bands. (**d**) Supershift assay using anti-YY1 antibody. After binding of the rs356219-A probe and SH-SY5Y nuclear extract in the gel shift assay, anti-YY1 antibody was added and analyzed by electrophoresis. The shift band (arrowhead) was supershifted by anti-YY1 antibody (arrow), confirming that the shift band contains YY1.

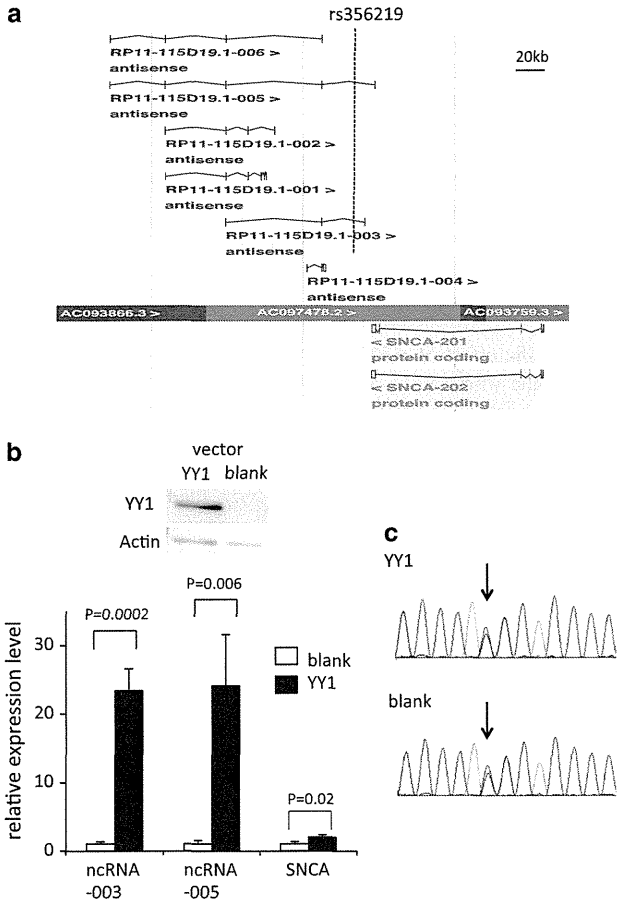

Figure 3 *SNCA* and its 3′-flanking ncRNA expression in YY1-transfected SH-SY5Y cells. (**a**) Genomic structure of *SNCA* and its 3′-flanking region (Ensemble Genome Browser). SNP rs356219 locates in intron of *RP11-115D19.1-003* and *-005* (dotted line). (**b**) Quantification of *SNCA* mRNA and two spliced isoforms of *RP11-115D19.1* ncRNA (*-003* and *-005*) in SH-SY5Y cells transfected by YY1 expression vector or blank vector. Overexpression of YY1 was confirmed by western blot analysis (upper). Three YY1 plates and three blank plates were quantified. Mean values of three YY1 plates (black bar) relative to the mean of three blank plates (white bar) are shown with s.d. (lower). YY1 transfection showed 23-fold increase in *RP11-115D19.1-003*, 24-fold increase in *RP11-115D19.1-005* and twofold increase in *SNCA* expression levels. (**c**) Semiquantitative analysis of allele-specific expression of *SNCA* 3′-UTR. Sequencing chromatograms of SH-SY5Y RT-PCR products of *SNCA* 3′-UTR containing rs356165 (arrow) are shown. Little difference between the heights of allele-C and allele-T was observed, both in the YY1 and blank transfection.

protective allele is not contradictory to YY1-stimulated expression of *RP11-115D19.1*.

SNCA, ncRNA *RP11-115D19.1* and *YY1* expression in relation to rs356219

We found the possibility that rs356219 may influence expression of *RP11-115D19.1* from *in vitro* and cellular experiments (Figures 1–3). To extend the findings, we investigated *SNCA* and *RP11-115D19.1* expression in relation to rs356219 genotypes in autopsied brain tissues. We previously reported that *SNCA* expression levels tended to be positively correlated with the number of the disease allele of rs7684318 in autopsied cortices.[13] Because rs356219 and rs7684318 are in a tight linkage disequilibrium group (Supplementary Table 3), our previous finding is to be replicated in relation to rs356219. Actually, rs356219 genotypes were completely correlated with those of rs7684318 in our autopsied samples. Moreover, we synthesized new cDNAs and quantified *SNCA* expression levels by real-time RT-PCR to compare among rs356219 genotypes. Although the difference among genotypes did not reach significance, we confirmed similar tendency with our previous report; mean of *SNCA* mRNA was lowest in AA (homozygote of protective alleles) either in cases, controls and combined (Supplementary Figure 2a). We also analyzed *RP11-*

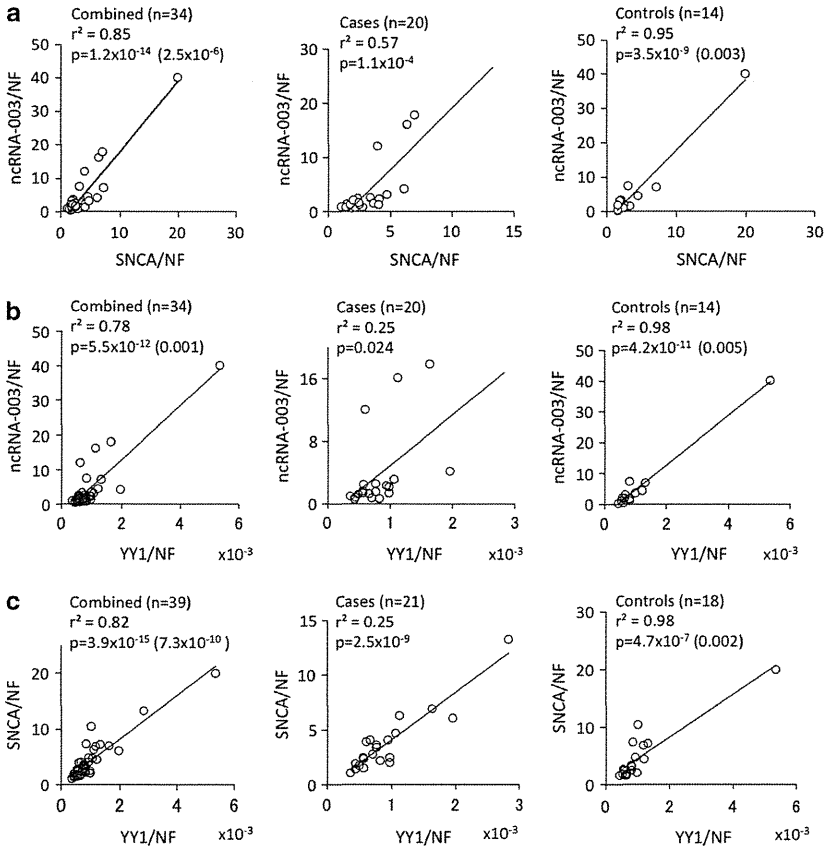

Figure 4 Correlation of SNCA, its 3′-flanking ncRNA and YY1 expression levels in autopsied frontal cortices. Scatterplots of *SNCA* versus *RP11-115D19.1-003* (**a**), *YY1* versus *RP11-115D19.1-003* (**b**) and *YY1* versus *SNCA* (**c**) expression levels (standardized by NF in arbitrary units). Plots are shown in all the samples (combined), cases and controls separately. Linear regression lines are indicated with r^2 and *P* values (Pearson's correlation analysis). Even after excluding the outliner in the controls, the strong correlations remain (*P*-values are in parenthesis).

115D19.1 expression in relation to rs356219. *RP11-115D19.1-005* expression levels in 38 out of the 39 cortices were too low to be quantified (data not shown); however, those of *RP11-115D19.1-003* could be quantified in 34 cortices. Compared with *SNCA*, mean values of *RP11-115D19.1-003* expression levels showed little difference among rs356219 genotypes (Supplementary Figure 2b). However, it was notable that *RP11-115D19.1-003* expression levels were strongly and positively correlated with those of *SNCA* (Figure 4a). Even after excluding the outliner in the controls, the strong correlation remained ($P = 2.5 \times 10^{-6}$ in combined and $P = 0.003$ in controls). We also examined *YY1* mRNA expression levels in cortical tissues. *YY1* expression levels were normalized by those of *NF*, because previous immunohistochemical study in an adult rodent brain reported that YY1 were strongly expressed in neurons and not detected in astrocytes.[21] *YY1* expression levels showed no significant difference among rs356219 genotype (Supplementary Figure 2c); however, positive correlation between *YY1* and *RP11-115D19.1-003* (Figure 4b) was compatible to the YY1-induced ncRNA expression shown in cellular YY1-overexpression experiment (Figure 3).

Effects of overexpression/knockdown of ncRNA *RP11-115D19.1* on *SNCA* expression in SH-SY5Y cells

Positive correlation between *SNCA* and *RP11-115D19.1* in the brain suggests regulatory roles of *RP11-115D19.1* on the *SNCA* expression. To address this issue, we investigated *SNCA* expression levels in SH-SY5Y cells transfected by *RP11-115D19.1* expressing vectors or siRNA designed from a common region of *RP11-115D19.1-003* and *-005*. Overexpression of *RP11-115D19.1* did not affect *SNCA* expression levels significantly (Figure 5a). On the contrary, siRNA-mediated knockdown (~90%) of *RP11-115D19.1* increased *SNCA* expression levels significantly (1.2-fold, $P = 0.0014$) (Figure 5b), which was replicated in three independent knockdown experiments (data not shown). These findings suggest that *RP11-115D19.1* may have repressive effect on the *SNCA* expression.

DISCUSSION

Recent GWAS have provided new information regarding PD susceptibility genes.[14,15] Our GWAS analysis in the Japanese population confirmed strong associations at *SNCA* and *LRRK2* and identified novel susceptibility loci, including *PARK16* (1q32) and *BST1* (4p15).[14] GWAS in individuals of European ancestry confirmed strong associations at *SNCA*, *MAPT* and *LRRK2*, and also confirmed *PARK16* as a novel locus.[15] Following meta-analysis of GWAS in the European ancestry populations confirmed *BST1* susceptibility.[22] Susceptibility associated with *MAPT* was not consistent between the populations, in part because of ethnic differences in allele frequencies. For example, a strong association for the H1/H2 haplotype of *MAPT* (OMIM 157140) has been reported in Caucasians,[23] but this observation has not been replicated in Asians. The frequency of the H2 haplotype is

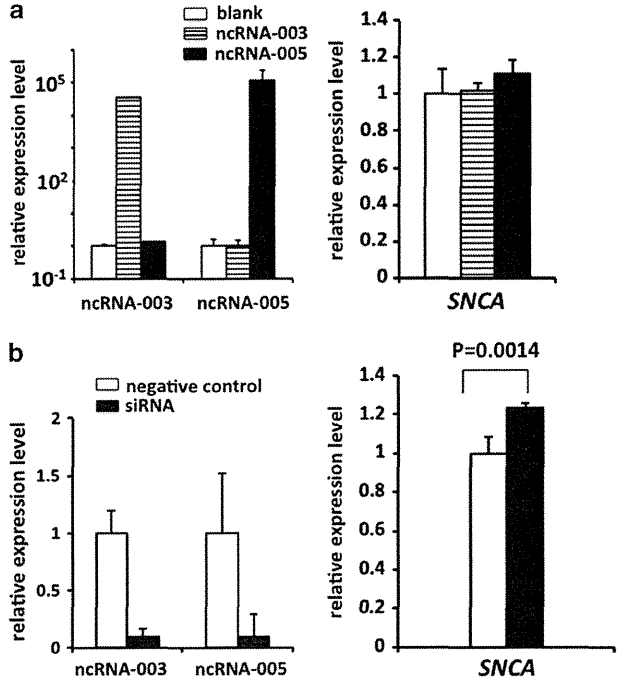

Figure 5 *SNCA* expression in SH-SY5Y cells after overexpression/knockdown of the ncRNA. (**a**) Quantification of *SNCA* mRNA in SH-SY5Y cells transfected by *RP11-115D19.1 ncRNA-003* and *-005* expression vectors or blank vector. Mean values of three *ncRNA-003* plates (striped bar) or three *ncRNA-005* (black bar) plates relative to the mean of three blank plates (white bar) are shown with s.d. Overexpression (over 10000-fold) of *ncRNA-003/-005* was confirmed (left). *SNCA* expression did not change significantly by transfection of *ncRNA-003* ($P=0.83$, versus blank, *t*-test) or *ncRNA-005* ($P=0.28$, versus blank, *t*-test) (right). (**b**) Quantification of *SNCA* mRNA in SH-SY5Y cells transfected by siRNA targeted to *RP11-115D19.1* or negative control RNA. Mean value of four siRNA plates (black bar) relative to the mean of four control plates (white bar) are shown with s.d. Repression of the *ncRNA-003/005* (~0.1-fold) was confirmed (left). *SNCA* expression increased significantly (~1.2-fold, $P=0.0014$, *t*-test) by transfection of siRNA (right).

approximately 20% in Caucasians but almost absent in Asians.[24] On the contrary, *SNCA*, *LRRK2*, *BST1* and *PARK16* susceptibilities are consistent in both the populations. To examine how SNPs might affect disease susceptibility, we focused on the *SNCA* SNPs that associate with PD across different ethnicities.

Of the four SNPs analyzed, only rs356219 showed distinct allele-specific features. The protective A allele showed greater activity in lucifersae assays than did the disease allele G. Moreover, specific binding of a nuclear protein to the protective A allele was observed using gel shift assays. When purified, this protein was identified as the transcription factor YY1, a ubiquitous zinc-finger transcription factor belonging to the Drosophila-Polycomb group protein family. The name Yin Yang 1 reflects its dual effects on transcriptional regulation, as YY1 can stimulate or repress gene expression depending on the cellular context. YY1 is associated with multiple biological functions such as proliferation, differentiation, apoptosis and tumorigenesis.[25,26] Comparison with known YY1 consensus binding motifs[27] supports the idea that the sequence of rs356219 would alter YY1 affinity in an allele-specific manner (Supplementary Figure 1). Based on the hypothesis that increased SNCA leads to LBD, it is reasonable to presume that YY1 could diminish *SNCA* gene expression levels by binding to the protective allele. However, elevated luciferase activity of the construct containing the rs356219-A protective allele seems contradictory. To address this issue, we transfected YY1 expression vector to human neuroblastoma cell line SH-SY5Y of which rs356219 genotype is GA and compared allele-specific expression level using 3′-UTR SNP rs356165 as a marker. YY1 was successfully overexpressed in SH-SY5Y and little difference of *SNCA* expression levels between the alleles was observed (Figure 3c), suggesting little possibility of allele-specific transcription regulation by YY1–rs356219 interaction, at least in SH-SY5Y cells. We raised another possibility that rs356219 might influence transcription of a certain gene regulating *SNCA* expression. Recent Ensemble Genome Browser (http://www.ensembl.org/) showed novel antisense ncRNA *RP11-115D19.1* in *SNCA* 3′-flanking region. We also investigated the expression of *RP11-115D19.1*, because rs356219 is located in introns of the two spliced isoforms, *RP11-115D19.1-003* and *-005* (Figure 3a). Surprisingly, *RP11-115D19.1* expression was prominently stimulated by YY1 overexpression, in contrast to the little change in *SNCA* expression (Figure 3b). From these findings, it would be informative to analyze *RP11-115D19.1* expression levels stimulated by YY1 in relation to rs356219 genotypes. Because no SNP was found in SH-SY5Y *RP11-115D19.1* exons, we designed an experiment to transfect YY1 expression vector to human lymphoblasts G or A in rs356219 and compare *SNCA* mRNA expression levels between G and A. However, because of low transfection efficiency (~10% by electroporation), we could not induce YY1 in lymphoblasts (data not shown).

Our *in vitro* and cellular experiments showed the possibility that rs356219 might influence YY1-stimulated transcription of *RP11-115D19.1*. To extend this, we investigated steady state *SNCA* and *RP11-115D19.1* expression levels in autopsied frontal cortices in relation to rs356219 genotypes. *SNCA* expression levels in cortices tended to be positively correlated with the number of the disease allele of rs356219 (Supplementary Figure 2a), replicating our previous result.[13] Our result was not consistent with other groups' previous reports. Fuchs *et al.*[28] reported that higher *SNCA* mRNA correlated with rs356219 disease allele in the substantia nigra of the midbrain, however, with the protective allele in the cerebellum. On the other hand, Linnertz *et al.*[29] reported that higher *SNCA* mRNA correlated with rs356219 protective allele in the temporal cortices and midbrain and unchanged among the genotypes in the frontal cortices. The discrepancies among these studies might be from the number and variation of samples.

We also analyzed steady state *in vivo* *RP11-115D19.1* expression levels and found little difference among genotypes (Supplementary Figure 2b). However, it was of note that *RP11-115D19.1* expression levels were strongly and positively correlated with those of *SNCA* (Figure 4a). Recent reports focused on SNP-coexpression associations.[30,31] We found a positive correlation between *SNCA* and *RP11-115D19.1* in either of the rs356219 genotype. The significance of correlation tended to increase according to the number of the disease allele G (Supplementary Figure 3). To confirm this tendency, large number of samples must be analyzed.

We also quantified *RP11-115D19-003* and *SNCA* mRNA levels in lymphoblasts originated from PD patients harboring GG and AA (Supplementary Figure 4). Similarly to the brain, there were no significant differences in *RP11-115D19-003* and *SNCA* expression levels between GG and AA lymphoblasts. In contrast to the brain, however, there was no significant correlation between *RP11-115D19-003* and *SNCA* levels in lymphoblasts. Although the numbers examined were limited, these results suggest interaction between *RP11-115D19* and *SNCA* expressions may be brain-specific.

The coexpression suggests functional interaction between the two genes. *RP11-115D19.1* transcripts span 0.4–1.8 kb, classified by size to long noncoding RNAs (lncRNAs).[32] Although the function of majority of lncRNAs remains uncovered, some are supposed to participate in regulating transcription of coding genes. For example, it was reported that mRNA of *BACE1*, *β-site APP (amyloid precursor protein) cleaving enzyme 1*, was stabilized by *BACE1* antisense transcript, a lncRNA including an exon complementary to a *BACE-1* exon.[33] On the contrary, recent work reported that *brain-derived neurotrophic factor* (*BDNF*) was repressed by its antisense RNA transcript.[34] These reports showed that some antisense ncRNAs downregulated and others upregulated transcription of the sense genes. *RP11-115D19.1-005* transcript overlaps *SNCA* 3′-UTR partly in tail-to-tail manner (Figure 3a), suggesting putative regulatory activity on *SNCA* expression. *RP11-115D19.1-005* transcript was hardly detected in steady state brain mRNA; however, it was prominently stimulated by YY1 in SH-SY5Y cells, as well as in *-003* transcript.

To investigate how *RP11-115D19.1* may influence *SNCA* expression, we performed cellular overexpression and knockdown experiments. We found that siRNA-mediated knockdown of the ncRNA increased *SNCA* expression (~ 1.2-fold) in SH-SY5Y cells (Figure 5b). The effect seems small; however, it could be sufficient to influence susceptibility to late-onset sporadic PD and DLB, caused by multiple genetic and environmental factors. The reason why overexpression of the ncRNA did not suppress *SNCA* expression remains unknown. We hypothesize that ncRNA may influence *SNCA* expression in a locus-dependent manner and that repressive effect may be saturated at endogeneous (low) expression level of ncRNA.

We performed similar analysis using human embryonic kidney-derived HEK293 cells. YY1-induced expression of ncRNA was replicated in HEK293 cells (Supplementary Figure 5). The degree of ncRNA stimulation in HEK293 cells, however, was smaller than those in SH-SY5Y cells. *SNCA* expression levels in HEK293 cells did not change significantly after YY1 overexpression, ncRNA overexpression or ncRNA knockdown. These suggest that ncRNA's repressive effect on *SNCA* expression may be specific to neuroblastoma cells.

Based on our demonstration that ncRNA has directly repressive effect on *SNCA* expression *in vitro*, positive correlation between *SNCA* and its antisense ncRNA *in vivo* may be explained as follows: One possibility is that expression of antisense ncRNA may coordinate with that of sense gene *SNCA* under locus-specific transcriptional regulation. Another possibility is that certain neurotoxic factors, including oxidative stress, may cause stimulation of *SNCA* and ncRNA expression levels simultaneously. Simultaneous stimulation of *SNCA* and *YY1* may be also possible, because of correlation of *SNCA* and *YY1* expression levels in the brain (Figure 4c) and YY1-induced expression of ncRNA in cells (Figure 3). In both the hypotheses (Supplementary Figure 6), ncRNA may be beneficial to maintain *SNCA* expression levels within normal range.

Accumulation of SNCA is thought to be neurotoxic. On the other hand, the protective effects of SNCA are also reported. Chandra *et al.*[35] reported that transgenic expression of *SNCA* rescued neurodegeneration in *CSPα* knockout mice. Musgrove *et al.*[36] reported that endogeneous SNCA upregulation in response to weak oxidative stress was neuroprotective against additional acute oxidative stress in primary cultured neurons. These suggest that SNCA exerts neuroprotective effects under disease or stress. However, repeated stresses or lasting disease state may cause SNCA accumulation. Extraordinary upregulation of SNCA may be also harmful. Therefore, *SNCA* expression levels must be fine-tuned to maintain proper range *in vivo*. To clarify the regulatory mechanism of the ncRNA, with or without neurotoxic stresses, further intensive approach should be necessary.

In conclusion, our findings of the protective-allele specific YY1 and antisense ncRNA raised a novel possible mechanism to regulate *SNCA* expression.

CONFLICT OF INTEREST

The authors declare no conflict of interest.

ACKNOWLEDGEMENTS

We are grateful to the individuals with PD who participated in this study. We also thank Dr Yoshitaka Nagai for helpful comments; Dr Kouichi Ozaki for technical comments of luciferase assay and gel shift assay; Dr Fumiko Hirose and Dr Isao Kuraoka for technical comments of protein purification by affinity beads; Dr Hidetoshi Inoko and Dr Katsushi Tokunaga for control samples; Dr Yoshihisa Watanabe for technical comments of electroporation; and Dr Jennifer Logan for editing the manuscript. This work was supported by a grant from the Core Research for Evolutional Science and Technology (CREST), Japan Science and Technology Agency (JST); by the Global COE program and KAKENHI (17019044 and 19590990), both from the Ministry of Education, Culture, Sports, Science and Technology of Japan; and by the Grant-in-Aid for 'The Research Committee for the Neurodegenerative Diseases' of the Research on Measures for Intractable Diseases and Research Grant (H19-Genome-Ippan-001), all from the Ministry of Health, Labor and Welfare of Japan.

1 de Rijk, M. C., Tzourio, C., Breteler, M. M., Dartigues, J. F., Amaducci, L., Lopez-Pousa, S. *et al.* Prevalence of parkinsonism and Parkinson's disease in Europe: the EUROPARKINSON Collaborative Study. European Community Concerted Action on the Epidemiology of Parkinson's disease. *J. Neurol. Neurosurg. Psychiatry* **62,** 10–15 (1997).
2 Shults, C. W. Lewy bodies. *Proc. Natl Acad. Sci. USA* **103,** 1661–1668 (2006).
3 Farrer, M. J. Genetics of Parkinson disease: paradigm shifts and future prospects. *Nat. Rev. Genet.* **7,** 306–318 (2006).
4 Lesage, S. & Brice, A. Parkinson's disease: from monogenic forms to genetic susceptibility factors. *Hum. Mol. Genet.* **18,** R48–R59 (2009).
5 Warner, T. T. & Schapira, A. H. Genetic and environmental factors in the cause of Parkinson's disease. *Ann. Neurol.* **53** (Suppl 3), S16–S23 (2003).
6 Polymeropoulos, M. H., Lavedan, C., Leroy, E., Ide, S. E., Dehejia, A., Dutra, A. *et al.* Mutation in the α-synuclein gene identified in families with Parkinson's disease. *Science* **276,** 2045–2047 (1997).
7 Spillantini, M. G., Schmidt, M. L., Lee, V. M., Trojanowski, J. Q., Jakes, R. & Goedert, M. α -Synuclein in Lewy bodies. *Nature* **388,** 839–840 (1997).
8 Singleton, A. B., Farrer, M., Johnson, J., Singleton, A., Hague, S., Kachergus, J. *et al.* α -Synuclein locus triplication causes Parkinson's disease. *Science* **302,** 841 (2003).
9 Miller, D. W., Hague, S. M., Clarimon, J., Baptista, M., Gwinn-Hardy, K., Cookson, M. R. *et al.* α-Synuclein in blood and brain from familial Parkinson disease with *SNCA* locus triplication. *Neurology* **62,** 1835–1838 (2004).
10 Chartier-Harlin, M. C., Kachergus, J., Roumier, C., Mouroux, V., Douay, X., Lincoln, S. *et al.* α-Synuclein locus duplication as a cause of familial Parkinson's disease. *Lancet* **364,** 1167–1169 (2004).
11 Ibanez, P., Bonnet, A. M., Debarges, B., Lohmann, E., Tison, F., Pollak, P. *et al.* Causal relation between α-synuclein gene duplication and familial Parkinson's disease. *Lancet* **364,** 1169–1171 (2004).
12 Mueller, J. C., Fuchs, J., Hofer, A., Zimprich, A., Lichtner, P., Illig, T. *et al.* Multiple regions of α-synuclein are associated with Parkinson's disease. *Ann. Neurol.* **57,** 535–541 (2005).
13 Mizuta, I., Satake, W., Nakabayashi, Y., Ito, C., Suzuki, S., Momose, Y. *et al.* Multiple candidate gene analysis identifies *α-synuclein* as a susceptibility gene for sporadic Parkinson's disease. *Hum. Mol. Genet.* **15,** 1151–1158 (2006).
14 Satake, W., Nakabayashi, Y., Mizuta, I., Hirota, Y., Ito, C., Kubo, M. *et al.* Genome-wide association study identifies common variants at four loci as genetic risk factors for Parkinson's disease. *Nat. Genet.* **41,** 1303–1307 (2009).
15 Simon-Sanchez, J., Schulte, C., Bras, J. M., Sharma, M., Gibbs, J. R., Berg, D. *et al.* Genome-wide association study reveals genetic risk underlying Parkinson's disease. *Nat. Genet.* **41,** 1308–1312 (2009).
16 Bower, J. H., Maraganore, D. M., McDonnell, S. K. & Rocca, W. A. Incidence and distribution of parkinsonism in Olmsted County, Minnesota, 1976-1990. *Neurology* **52,** 1214–1220 (1999).
17 Adachi, O., Kawai, T., Takeda, K., Matsumoto, M., Tsutsui, H., Sakagami, M. *et al.* Targeted disruption of the *MyD88* gene results in loss of IL-1- and IL-18-mediated function. *Immunity* **9,** 143–150 (1998).

18 Ozaki, K., Ohnishi, Y., Iida, A., Sekine, A., Yamada, R., Tsunoda, T. *et al.* Functional SNPs in the lymphotoxin-α gene that are associated with susceptibility to myocardial infarction. *Nat. Genet.* **32,** 650–654 (2002).
19 Kuruma, H., Egawa, S., Oh-Ishi, M., Kodera, Y., Satoh, M., Chen, W. *et al.* High molecular mass proteome of androgen-independent prostate cancer. *Proteomics* **5,** 1097–1112 (2005).
20 Rappsilber, J., Ishihama, Y. & Mann, M. Stop and go extraction tips for matrix-assisted laser desorption/ionization, nanoelectrospray, and LC/MS sample pretreatment in proteomics. *Anal. Chem.* **75,** 663–670 (2003).
21 Rylski, M., Amborska, R., Zybura, K., Konopacki, F. A., Wilczynski, G. M. & Kaczmarek, L. Yin Yang 1 expression in the adult rodent brain. *Neurochem. Res.* **33,** 2556–2564 (2008).
22 International Parkinson Disease Genomics Consortium, Nalls, M. A., Plagnol, V., Hernandez, D. G., Sharma, M., Sheerin, U. M. *et al.* Imputation of sequence variants for identification of genetic risks for Parkinson's disease: a meta-analysis of genome-wide association studies. *Lancet* **377,** 641–649 (2011).
23 Zabetian, C. P., Hutter, C. M., Factor, S. A., Nutt, J. G., Higgins, D. S., Griffith, A. *et al.* Association analysis of *MAPT* H1 haplotype and subhaplotypes in Parkinson's disease. *Ann. Neurol.* **62,** 137–144 (2007).
24 Stefansson, H., Helgason, A., Thorleifsson, G., Steinthorsdottir, V., Masson, G., Barnard, J. *et al.* A common inversion under selection in Europeans. *Nat. Genet.* **37,** 129–137 (2005).
25 Shi, Y., Lee, J. S. & Galvin, K. M. Everything you have ever wanted to know about Yin Yang 1..... *Biochim. Biophys. Acta* **1332,** F49–F66 (1997).
26 Gordon, S., Akopyan, G., Garban, H. & Bonavida, B. Transcription factor YY1: structure, function, and therapeutic implications in cancer biology. *Oncogene* **25,** 1125–1142 (2006).
27 Shrivastava, A. & Calame, K. An analysis of genes regulated by the multi-functional transcriptional regulator Yin Yang-1. *Nucleic Acids Res.* **22,** 5151–5155 (1994).
28 Fuchs, J., Tichopad, A., Golub, Y., Munz, M., Schweitzer, K. J., Wolf, B. *et al.* Genetic variability in the *SNCA* gene influences α-synuclein levels in the blood and brain. *FASEB J.* **22,** 1327–1334 (2008).
29 Linnertz, C., Saucier, L., Ge, D., Cronin, K. D., Burke, J. R., Browndyke, J. N. *et al.* Genetic regulation of α-synuclein mRNA expression in various human brain tissues. *PLoS One* **4,** e7480 (2009).
30 Kayano, M., Takigawa, I., Shiga, M., Tsuda, K. & Mamitsuka, H. Efficiently finding genome-wide three-way gene interactions from transcript- and genotype-data. *Bioinformatics* **25,** 2735–2743 (2009).
31 Wang, Y., Joseph, S. J., Liu, X., Kelley, M. & Rekaya, R. SNPxGE^2: a database for human SNP-coexpression associations. *Bioinformatics* **28,** 403–410 (2012).
32 Costa, F. F. Non-coding RNAs: meet thy masters. *Bioessays* **32,** 599–608 (2010).
33 Faghihi, M. A., Modarresi, F., Khalil, A. M., Wood, D. E., Sahagan, B. G., Morgan, T. E. *et al.* Expression of a noncoding RNA is elevated in Alzheimer's disease and drives rapid feed-forward regulation of β-secretase. *Nat. Med.* **14,** 723–730 (2008).
34 Modarresi, F., Faghihi, M. A., Lopez-Toledano, M. A., Fatemi, R. P., Magistri, M., Brothers, S. P. *et al.* Inhibition of natural antisense transcripts in vivo results in gene-specific transcriptional upregulation. *Nat. Biotechnol.* **30,** 453–459 (2012).
35 Chandra, S., Gallardo, G., Fernández-Chacón, R., Schlüter, O. M. & Südhof, T. C. α-synuclein cooperates with CSPα in preventing neurodegeneration. *Cell* **123,** 383–396 (2005).
36 Musgrove, R. E. J., King, A. E. & Dickson, T. C. Neuroprotective upregulation of endogeneous alpha-synuclein precedes ubiquitination in cultured dopaminergic neurons. *Neurotox. Res.* **19,** 592–602 (2011).

Supplementary Information accompanies the paper on Journal of Human Genetics website (http://www.nature.com/jhg)

SCIENTIFIC REPORTS

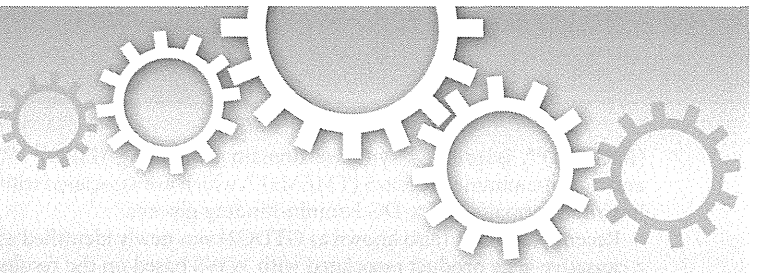

OPEN

SUBJECT AREAS:
GLYCOBIOLOGY
TRANSFERASES

Received
4 September 2013

Accepted
5 November 2013

Published
21 November 2013

Correspondence and requests for materials should be addressed to S.O. (shogo@hs.med.kyoto-u.ac.jp) or K.K. (kkato@phar.nagoya-cu.ac.jp)

* These authors contributed equally to this work.

AGO61-dependent GlcNAc modification primes the formation of functional glycans on α-dystroglycan

Hirokazu Yagi[1]*, Naoki Nakagawa[2]*, Takuya Saito[1], Hiroshi Kiyonari[3], Takaya Abe[3], Tatsushi Toda[4], Sz-Wei Wu[5], Kay-Hooi Khoo[5], Shogo Oka[2] & Koichi Kato[1,6]

[1]Graduate School of Pharmaceutical Sciences, Nagoya City University, 3-1 Tanabe-dori, Mizuho-ku, Nagoya 467-8603, Japan, [2]Department of Biological Chemistry, Human Health Sciences, Graduate School of Medicine, Kyoto University, 53 Kawahara-cho, Shogoin, Sakyo-ku, Kyoto 606-8507, Japan, [3]Laboratory for Animal Resources and Genetic Engineering, RIKEN Center for Developmental Biology, 2-2-3 Minatojima Minami, Chuou-ku, Kobe 650-0047, Japan, [4]Division of Neurology/Molecular Brain Science, Kobe University Graduate School of Medicine, 7-5-1 Kusunoki-chou Chuo-ku, Kobe 650-0017, Japan, [5]Institute of Biological Chemistry, Academia Sinica, 128, Academia Road Sec 2, Nankang, Taipei 115, Taiwan, [6]Okazaki Institute for Integrative Bioscience and Institute for Molecular Science, National Institutes of Natural Sciences, 5-1 Higashiyama Myodaiji, Okazaki 444-8787, Japan.

Dystroglycanopathy is a major class of congenital muscular dystrophy that is caused by a deficiency of functional glycans on α-dystroglycan (α-DG) with laminin-binding activity. A product of a recently identified causative gene for dystroglycanopathy, AGO61, acted *in vitro* as a protein *O*-mannose β-1,4-*N*-acetylglucosaminyltransferase, although it was not functionally characterized. Here we show the phenotypes of AGO61-knockout mice and demonstrate that AGO61 is indispensable for the formation of laminin-binding glycans of α-DG. AGO61-knockout mouse brain exhibited abnormal basal lamina formation and a neuronal migration defect due to a lack of laminin-binding glycans. Furthermore, our results indicate that functional α-DG glycosylation was primed by AGO61-dependent GlcNAc modifications of specific threonine-linked mannosyl moieties of α-DG. These findings provide a key missing link for understanding how the physiologically critical glycan motif is displayed on α-DG and provides new insights on the pathological mechanisms of dystroglycanopathy.

Congenital muscular dystrophies and limb-girdle muscular dystrophies are clinically and genetically heterogeneous degenerative diseases that primarily affect voluntary muscles. Dystroglycanopathy is a group of these diseases associated with brain and eye abnormalities at the severe end of the clinical spectrum, including Walker–Warburg syndrome (WWS), muscle-eye-brain (MEB) diseases, Fukuyama-type congenital muscular dystrophy (FCMD), and congenital muscular dystrophy type 1D (MDC1D). The hallmark of these diseases is hypoglycosylation of α-dystroglycan (α-DG)[1,2], which along with β-DG is cleaved from a precursor protein encoded for by a single gene by post-translational processing[3]. A dystrophin glycoprotein complex that is formed from several intracellular, transmembrane, and extracellular proteins including α- and β-DG subunits connects the cytoskeleton of a muscle fiber to surrounding extracellular matrix components, such as laminin, agrin, and perlecan, depending on the glycosylation status of α-DG[4,5].

To date, 13 genes have been identified that are associated with dystroglycanopathies, among which 8 genes have been characterized as those encoding enzymes responsible for the formation of the functional α-DG glycans. Protein *O*-mannosyltransferase 1 (POMT1)[6], POMT2[7,8], and protein *O*-mannose β-1,2-*N*-acetylglucosaminyltransferase 1 (POMGnT1)[9] along with GDP-mannose pyrophosphorylase (GMPPB)[10] are involved in the biosynthesis of *O*-mannosyl glycans on α-DG. The outer regions of laminin-binding glycans consist of Xyl-GlcA repeat sequences, the formation of which is catalyzed by like-acetylglucosaminyltransferase (LARGE), a causative gene product for MDC1D[11,12]. Furthermore, phosphorylated *O*-mannosylation was identified on recombinant α-DG, the laminin-binding glycans of which were shown to be degraded by HFaq treatment that hydrolyzes phosphoester linkages[13]. Thus, the laminin-binding region is presumably linked to α-DG through post-phosphoryl *O*-manosylation. However, the functionally relevant glycan structure of α-DG has not been well delineated, notwithstanding that several mutants associated with dystroglycanopathy have been identified in fukutin[14], fukutin-related protein (FKRP)[15], UDP-GlcNAc:βGal β-1,3-*N*-acetylglucosaminyltransferase 1

(B3GNT1)[16], isoprenoid synthase domain containing (ISPD)[17–19], and transmembrane protein 5 (TMEM5)[19], which are associated with impaired formation of α-DG laminin-binding glycans.

Recently, AGO61 (also known as GTDC2) was newly identified as a causative gene product associated with WWS based on the results of whole-exome sequencing, homozygosity mapping, and morpholino-mediated knockdown of an AGO61 zebrafish ortholog[20]. It was subsequently characterized as a protein *O*-mannose β-1,4-*N*-acetylglucosaminyltransferase (POMGnT2) based on its *in vitro* enzymatic activities against a synthetic peptide substrate carrying a single *O*-Man[21]. Although a further β3GalNAc-extended and phosphorylated GlcNAcβ1-4Man-*O*- unit by β-1,3-*N*-acetylgalactosaminyltransferase 2 (B3GALNT2)[21,22] and protein kinase-like protein SGK196[21,23], respectively, was inferred to be essential for the formation of functional laminin binding glycans on αDG, the precise roles of AGO61 *in vivo* remain to be determined. Here, we characterized the phenotypes of AGO61-knockout mice and determined that AGO61 mediated the formation of laminin-binding glycans on α-DG.

Results

AGO61-knockout mice exhibit abnormal neuronal migration. We subjected the mouse AGO61 locus to targeted disruption. A null allele was generated by replacing the first coding exon with a neomycin resistance gene (Supplementary Fig. S1a). Mice that were heterozygous for the AGO61 mutation appeared grossly normal and were fertile. The progeny of a heterozygous intercross had an approximately 1 : 2 : 1 ratio of wild type and heterozygous AGO61, and a homozygous AGO61 ratio that was indicative of Mendelian inheritance. However, the newborns of homozygotes were slightly smaller than the other genotypes and died within the first day of birth (Fig. 1a and b).

AGO61 is mainly expressed in the central nervous system[20]. AGO61-knockout mouse brains exhibited abnormal basal lamina formation and the radial glia endfoot had detached from the basal membrane (Fig. 1c). Moreover, nuclear staining revealed defects in neuronal migration and laminar organization in the AGO61-KO mouse cerebral cortex (Fig. 1c). These neurodevelopmental abnormalities are commonly seen in dystroglycanopathy mouse models[24–26], which suggested an essential role for AGO61 in the functional maturation of α-DG *in vivo*.

AGO61 is indispensable for the formation of laminin-binding glycans of α-DG. For biochemical analysis, we enriched DG from mouse embryonic brains (embryonic day 17.5) with wheat germ agglutinin (WGA) beads and then performed laminin overlay and Western blot analyses using IIH6, which recognizes laminin-binding glycans on α-DG, and anti-α-DG core antibodies. AGO61-KO embryonic mouse brains exhibited α-DG hypoglycosylation, which indicated a lack of laminin-binding glycans (Fig. 2a). An immunoreactive band of an α-DG core of AGO61-KO mice migrated to a position similar to that of control mouse α-DG treated with HFaq (Fig. 2b). Furthermore, there were no significant differences between WT and KO mice brains in the expression levels of other dystroglycanopathy-associated genes (Fig. 2c). These results indicated that AGO61 was involved in the formation of laminin-binding glycans on α-DG.

To confirm these findings, we expressed the AGO61 protein in *AGO61*-deficient mouse embryonic fibroblasts (MEFs). AGO61 protein expression rescued the defect in laminin-binding glycans, whereas mutants with alleles associated with WWS (R158H and R445stop)[20] had no rescue capability (Fig. 2d). Although it has been reported that several dystroglycanopathy models with mutations in POMGnT1, LARGE, or fukutin could be recovered by LARGE overexpression, laminin-binding glycans were not rescued by LARGE overexpression in AGO-deficient MEFs (Fig. 2e). LARGE is located in the Golgi apparatus and is responsible for the formation of the

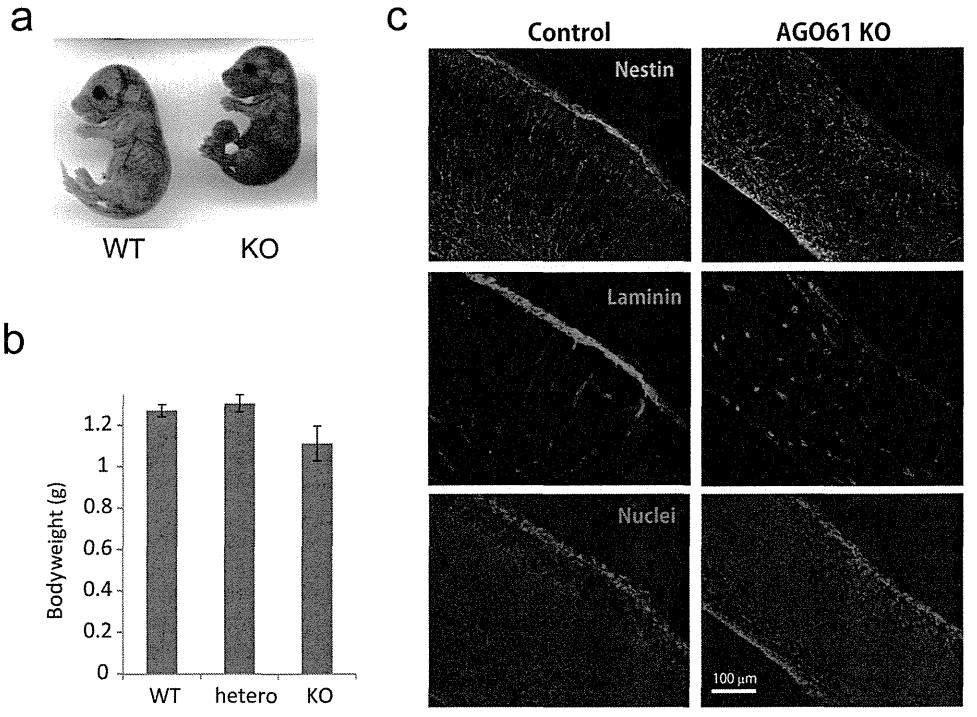

Figure 1 | AGO61-KO mice exhibit neuron migration defects. (a) Phenotypes of AGO61 KO and WT pups at embryonic day 17.5. (b) Body weights of wild type (WT), heterozygous (hetero), and KO pups at postnatal day 0 (n = 4–6 for each genotype). Results are means ± SDs. (c) Brain sagittal sections from AGO61-KO and WT pups at embryonic day 17.5 were stained with anti-nestin and anti-laminin antibodies used as primary antibodies, and then with Alexa Fluor 488-conjugated anti-rat IgG (*green*) and Alexa Fluor 595-conjugated anti-rabbit IgG (*red*) used as secondary antibodies, respectively. Nuclei were stained with DAPI (*blue*).

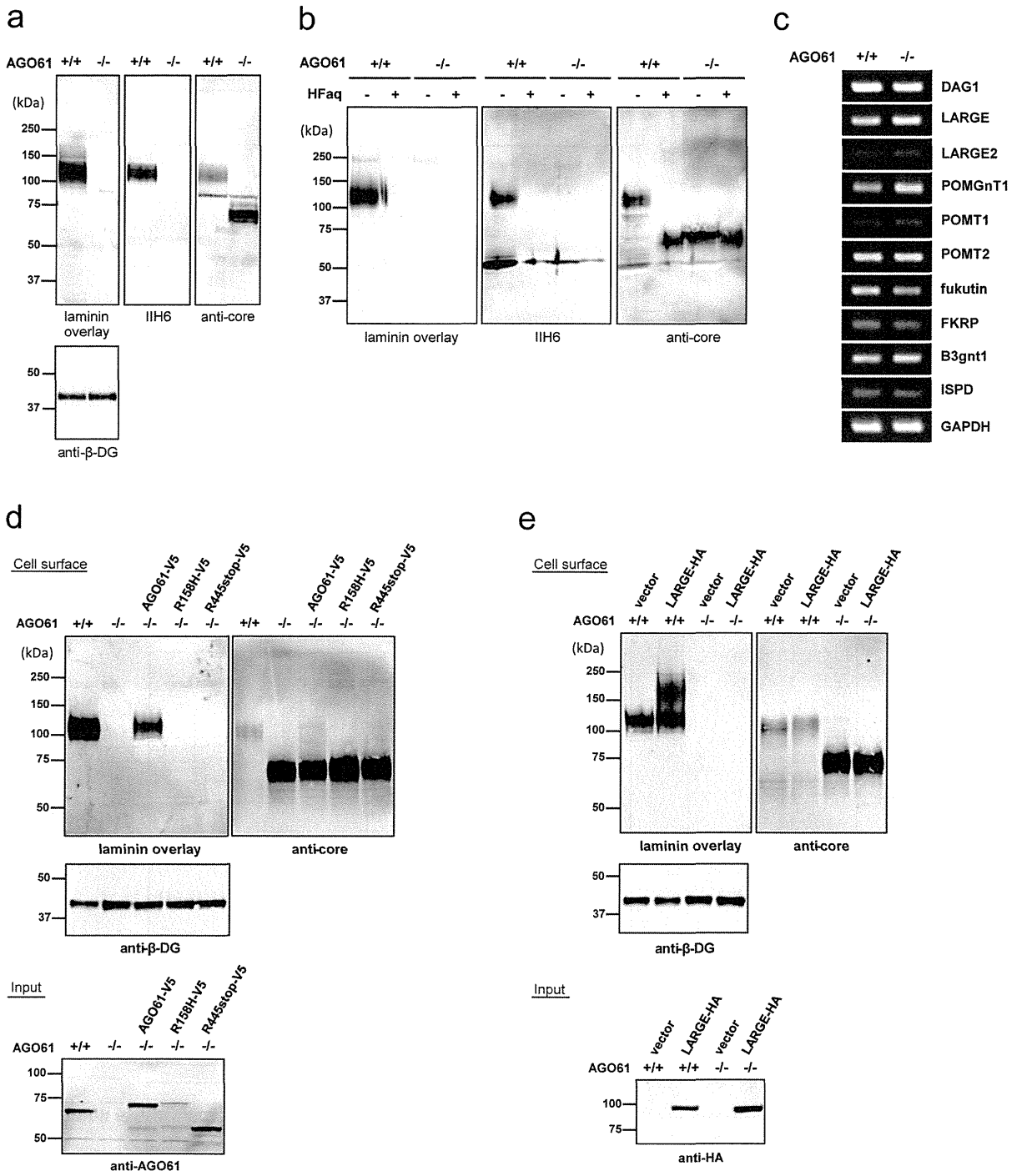

Figure 2 | AGO61 is indispensable for the formation of laminin-binding glycans of α-DG. (a) WGA-enriched brain lysates prepared from WT and AGO61-KO pups at embryonic day 17.5 were subjected to laminin overlay and immunoblot analysis using IIH6, anti α-DG core, and anti-β-DG antibodies. The full-length blot with anti-β-DG antibody is presented in Supplementary Fig. S7a. (b) Chemical dephosphorylation of α-DG from WGA enriched brain lysates. Brain lysates were treated with HFaq and then analyzed by laminin overlay and Western blot using IIH6 and anti α-DG core antibodies. (c) mRNA expression of DAG1, LARGE, LARGE2, POMGnT1, POMT1, POMT2, fukutin, FKRP, B3GNT1, ISPD, and GAPDH in brain tissue from WT and AGO61 KO pups at embryonic day 17.5 were analyzed by RT-PCR. GAPDH was used as an internal control. (d) AGO61 and its mutants with loss-of-function mutations were transfected into *AGO61*-deficient MEFs. Cell surface proteins were biotinylated, pull down, and analyzed by laminin overlay and Western blot with anti α-DG core and β-DG antibodies. Cell lysates were also analyzed for AGO61 expression by Western blot using an anti-AGO61 antibody. The full-length blots with anti-β-DG and anti-AGO61 antibodies are presented in Supplementary Figs. S7b and S7c, respectively. (e) LARGE was transfected into control (+/+) or AGO61-deficient (−/−) MEFs. Cell surface proteins were biotinylated, pulled down, and analyzed by laminin overlay and Western blot using anti α-DG core and β-DG antibodies. Cell lysates were analyzed for LARGE-HA expression by Western blot using an anti-HA antibody. The full-length blots with anti-β-DG and anti-HA antibodies are presented in Supplementary Figs. S7d and S7e, respectively.

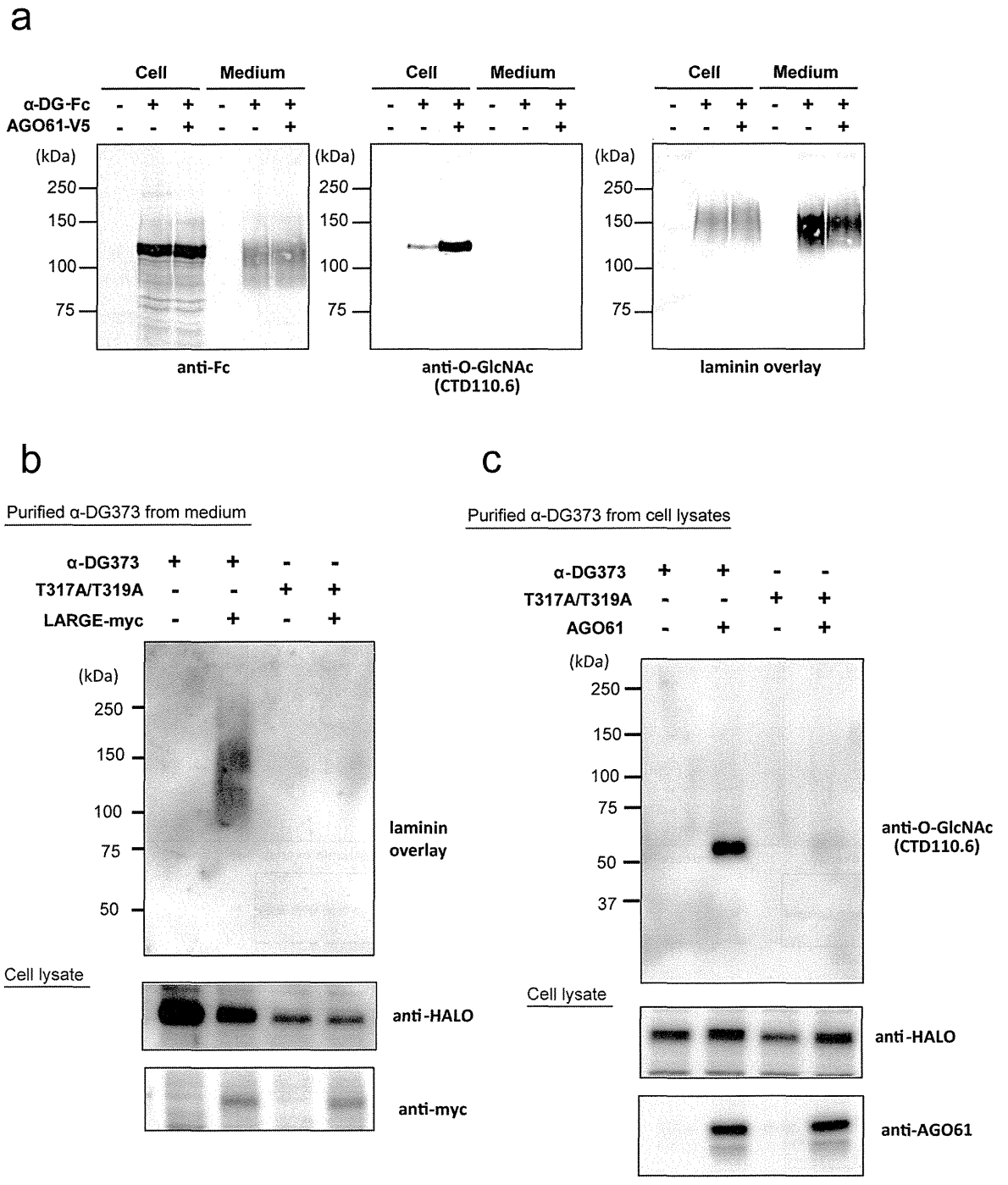

Figure 3 | AGO61 modifies GlcNAc residues at specific sites on α-DG. (a) α-DG-Fc was transiently transfected with or without AGO61 into COS1 cells. α-DG-Fc recombinant proteins were collected from cell lysates and culture media using protein A resin and analyzed for laminin overlay and Western blot using anti-Fc and anti-*O*-GlcNAc antibodies. (b) α-DG373-HALO and its mutant T317A/T319A were transiently transfected with or without LARGE-myc into COS7 cells. HALO-fused proteins were collected from medium using HALO resin followed by digestion with TEV protease and then analyzed by laminin overlay. Cell lysates were analyzed for the expression of HALO-fused proteins and LARGE-myc by Western blot using anti-HALO and anti-myc antibodies. The full-length blots with anti-HALO and anti-myc antibodies are presented in Supplementary Figs. S7f and S7g, respectively. (c) α-DG373-HALO and its mutant T317A/T319A were transiently transfected with or without AOG61 into COS7 cells. HALO-fused proteins were collected from the cell lysates using HALO resin followed by digestion with TEV protease and then analyzed by Western blot using an anti-*O*-GlcNAc antibody (CTD110.6). The cell lysates were analyzed for the expression of HALO-fused proteins and AGO61 by Western blot using anti-HALO and anti-AGO61 antibodies. The full-length blots with anti-HALO and anti-AGO61 antibodies are presented in Supplementary Figs. S7h and S7i, respectively.